Analytical approach to phonons and electron-phonon interactions in single-walled armchair carbon nanotubes

B. S. Kandemir and T. Altanhan
Department of Physics, Faculty of Sciences, Ankara University, 06100 Tandoğan, Ankara, Turkey
(Received 25 May 2007; revised manuscript received 16 November 2007; published 25 January 2008)

Phonon spectra are calculated in single-walled armchair carbon nanotubes within a mass and spring model. Classical Hamiltonian for the lattice vibrations that include nearest-neighbor, next-nearest-neighbor, and bond bending interactions has been quantized in the usual way, and then the phonon Hamiltonian is diagonalized by canonical transformations. Resolvent formalism is used to obtain phonon frequencies in analytical forms, where a procedure of the Fano problem is employed to choose correct phonon modes. The force constants are chosen from previous works, and the Raman mode at 1600 cm^{-1} is set to obtain the other modes. The electron-phonon interaction is investigated by phonon modulation of the hopping interaction, where the same canonical transformations are used in accordance with the phonon part. The electron-phonon coupling strengths in intraband and interband scattering for all modes within nearest-neighbor and radial bond bending interactions are found in terms of the q wave vectors and other parameters. Further, a different approach for the diagonalization of the electronic part arising from the tight-binding Hamiltonian is also presented in accordance with the electron-phonon interaction part.

DOI: 10.1103/PhysRevB.77.045426 PACS number(s): 63.22.−m, 81.07.De, 73.63.Fg, 63.20.D−

I. INTRODUCTION

The discovery of carbon nanotubes[1] in 1991 and then their syntheses[2,3] in 1993 have stimulated extensive investigations, both experimentally and theoretically, on the physical properties of these novel materials.[4] Since the observation of superconductivity in nanotubes[5] and nanotube ropes,[6] electron-phonon interactions and superconductivity[7] have been a focus of interest in these one-dimensional systems.

Electron-phonon interaction plays a pivotal role in understanding electronic, optical, and transport properties of carbon nanotubes. This interaction is closely associated with phonons, and therefore it is essential to know phonon spectra in every respect. Early works on the subject are based on the zone-folding method,[8,9] which is not a good approximation for the phonons because it fails, especially in the low-frequency region, to give correct nature of the modes.[10] There exist some models predicting two acoustical modes, longitudinal and torsional, which increase linearly and a doubly degenerate flexure mode, increasing as a square of the wave vector near the Γ point: These are Born's perturbation technique within a lattice dynamical model[11] and continuum model.[10,12] Recent studies of the graphene and single-walled carbon nanotube (SWCNT), based on the model of lattice dynamics with force-constant matrix,[13] an *ab initio* supercell approach,[14] and pseudopotential-density-functional theory[15] reveal these four acoustical phonon modes but only the graphene shows quadratically dispersed flexure mode near the Γ point. This discrepancy in nanotubes arises from the fact that calculations using potential functions that violate certain symmetry rules fail to give flexure modes.[16] Symmetry groups of SWCNTs are identified as line or rod groups[17] and are successfully applied to lattice dynamics of SWCNT in recent works, in which a symmetry-based force-constant approach[18–20] is used to obtain phonon spectra. In a more recent work,[21] the symmetry analysis is considered in rotational and translational invariance of the vibrational potential for the lattice dynamics of SWCNT, where the dispersion of the acoustic and flexure modes is precisely calculated in the low-frequency region.

Raman and infrared spectroscopies reveal the unusual electronic and phonon properties of SWCNTs and have been extensively studied,[22–24] and their classifications according to nanotubes symmetries are given in a recent work.[25] The best known Raman-active mode is the radial breathing mode which is unique to SWCNTs, and its frequency is proportional to the inverse diameter of the tube.[26]

First electron-phonon interaction studies in nanotubes are achieved by employing the tight-binding model for the interaction of electrons with acoustical phonons[27] and for linear electron-phonon coupling displaying a deformation type of approximation.[28] Scattering by optical phonons is important for transport properties and for the major source of broadening for certain Raman peaks.[29] The first attempt to calculate the interaction of an electron with acoustical and optical phonons is achieved by assuming phonon modulation of the hopping interaction in armchair and zigzag nanotubes.[30] Recently, the electron-phonon matrix element in SWCNTs is developed within the tight-binding approach based on density functional theory[31] and in order to study its effect on the Raman intensity[32] and intraband electron-phonon scattering.[33]

The aim of the present paper is to obtain the Hamiltonian of a system of electrons and phonons in armchair tubes, namely, as $H=H_0+H_{el\text{-}ph}^{tot}$, where the first term is a noninteracting part and consists of the sum of electron and phonon energies, expressed in the form $H_0=H_{el}+H_{ph}$,

$$H_0 = J_0 \sum_{j\equiv(m\ell)} \sum_{\delta_i} [C_{B,j+\delta_i}^{\dagger} C_{A,j} + C_{A,j}^{\dagger} C_{B,j+\delta_i}] + \sum_{\boldsymbol{q}\equiv(q,\alpha)} \sum_{i} \hbar\tilde{\omega}_i(\boldsymbol{q}) \left(a_{\boldsymbol{q}i}^{\dagger} a_{\boldsymbol{q}i} + \frac{1}{2} \right).$$

Here, the first term is the well-known spinless tight-binding Hamiltonian with a hopping parameter $J_0=2.4-3.1$ eV, wherein the terms in the brackets represent hopping of an electron from the carbon atom A to its three nearest-neighbor B atoms or vice versa, respectively. The second one is the dispersion for phonons in armchair SWCNTs. For a (n,n) armchair SWCNT, it has only $n+1$ component at each i which takes six values, since two different carbon atoms in the unit cell of the graphene have six degrees of freedom. Therefore, we have 6 $(n+1)$ distinct phonon branches, and they are all calculated analytically in the framework of the theory developed here.

In the present paper, as well as phonon frequencies $\tilde{\omega}_i(\boldsymbol{q})$, we give full analytical expressions for their corresponding electron-phonon interaction amplitudes. In Sec. II, the coordinates for the description of the model are summarized. In Sec. III, the lattice vibrations are treated classically at first, and then the quantization procedure is introduced. Through canonical transformations and resolvent formalism, the phonon frequencies are obtained analytically in this section. In Sec. IV, the electron-phonon interactions are investigated and the full Hamiltonian is obtained. The paper ends with a conclusion section.

II. COORDINATES

We are only concerned, throughout this work, with the phonon dispersion relations and their associated electron-phonon interactions in SWCNTs having armchair geometry, based on a model which is originally suggested by Mahan.[30] We construct and realize our model so as to be compatible with Mahan's arguments, dependent on the armchair geometry.[34] Therefore, it is quite instructive, from our point of view, to start with his coordinate description. An ideal nanotube can be thought of as a honeycomb lattice of carbon atoms that has been rolled up to make a seamless cylinder. It appears that the two-dimensional (2D) hexagonal lattice has two types of carbon atoms, A and B, which are separated by a distance a between neighboring atoms. While the unit cell of the 2D hexagonal lattice contains two carbon atoms, in the case of the nanotube, this number is increased considerably, depending on the chirality.[4] Let R be the radius of the tube; then we introduce two angles which are very useful throughout our investigations: the angle θ_1 between A and B atoms along the circumference and the angle θ_2 between A and B atoms that are first neighbors but displaced along the z direction. Both angles can be seen in Fig. 1. It should be stated here that the present approach is valid for SWCNTs with large radius, i.e., for tubes wherein the relation $\theta_1 \approx a/R$ holds. There are also considerations of electron-phonon interactions in ultrasmall-radius carbon nanotubes[35] within the framework of an empirical tight-binding method. Furthermore, it is assumed that the nanotube has a finite length that is much larger than its diameter so that the caps of the tubes can be neglected.

The lattice coordinates of a two-dimensional graphene plane are defined by the vectors $\boldsymbol{R}_{ij}=i\boldsymbol{a}_1+j\boldsymbol{a}_2$ with integer i and j, where $\boldsymbol{a}_1=\sqrt{3}a(\sqrt{3}/2,1/2)$ and $\boldsymbol{a}_2=\sqrt{3}a(\sqrt{3}/2,-1/2)$ are the base vectors, as shown in a (x,y) coordinate system

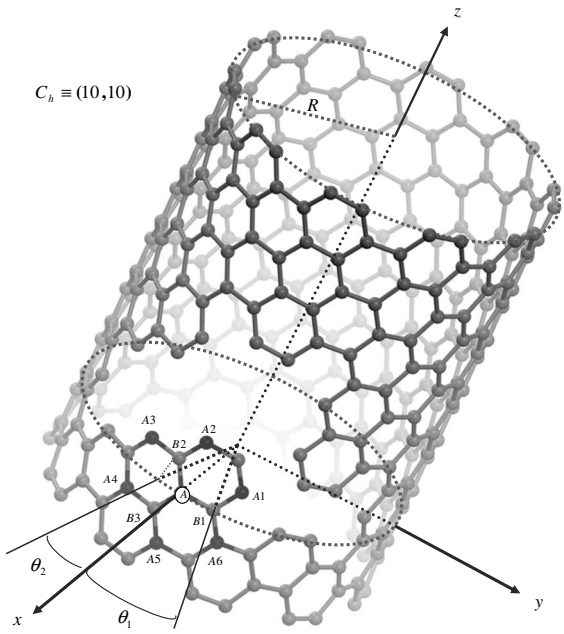

FIG. 1. A three-dimensional plot of a (10,10) armchair SWCNT showing the nearest- and next-nearest neighbors of carbon atom A with the related angles used in the text.

in Fig. 2, whose magnitude is the lattice constant of graphene, i.e., $\sqrt{3}a$, where a is the nearest-neighbor distance between two carbon atoms, i.e., $a=a_{\text{C-C}}=1.42$ Å. When this plane is rolled up[34] into a cylinder to form an armchair tube (n,n), the coordinates are to be designated by $\boldsymbol{R}_{\ell m}=\ell\boldsymbol{a}_1+m(\boldsymbol{a}_1+\boldsymbol{a}_2)$, where the integer ℓ denotes the position along the z axis and takes the values of $\ell=0,1,\ldots,N$, where N is the number of the atomic layers along the z axis and m labels the carbon atoms along the circumference of the tube and takes the values of $m=0,1,\ldots,n-1$,[30] wherein the linear ℓ and angular m quasimomenta quantum numbers are introduced. Instead, quantum numbers $\tilde{\ell}$ and $\tilde{m}$ of helical and pure angular momentum may be used to assign both elec-

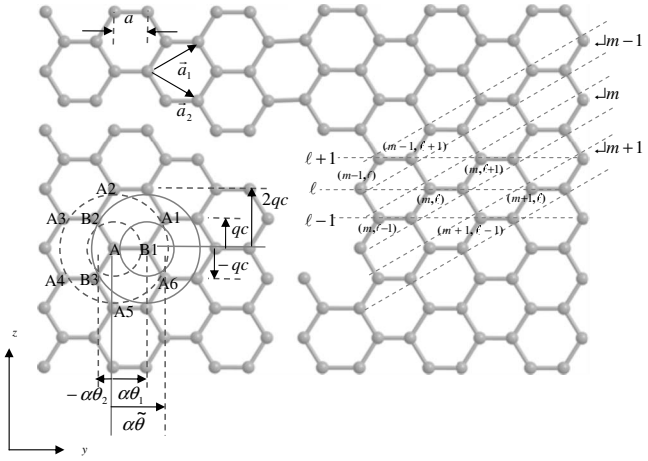

FIG. 2. Graphical picture of how the atomic layers of the graphene are labeled. Graphical illustrations of nearest- and next-nearest neighbors of A ($B1$) atoms are also given in the same picture together with the relevant phases.

tronic and phonon band structures.[34,36] Two sets of quantum numbers are biuniquely related.[19] In order to express the positions of any carbon atoms on tubes in (x,y,z) coordinates, we introduce an angle $\theta_{m\ell}=(2m+\ell)(\theta_1+\theta_2)$ such that an A type of atom is located at the point

$$\boldsymbol{R}_{A,m\ell}=[R\cos(\theta_{m\ell}),R\sin(\theta_{m\ell}),c\ell], \tag{1}$$

and three nearest-neighbor B-type atoms at

$$\boldsymbol{R}_{B,m\ell}=[R\cos(\theta_{m\ell}+\theta_1),R\sin(\theta_{m\ell}+\theta_1),c\ell],$$

$$\boldsymbol{R}_{B,m-1,\ell+1}=[R\cos(\theta_{m\ell}-\theta_2),R\sin(\theta_{m\ell}-\theta_2),c(\ell+1)],$$

$$\boldsymbol{R}_{B,m,\ell-1}=[R\cos(\theta_{m\ell}-\theta_2),R\sin(\theta_{m\ell}-\theta_2),c(\ell-1)], \tag{2}$$

and six next-nearest-neighbor A-type atoms at

$$\boldsymbol{R}_{A,m,\ell\mp1}=[R\cos(\theta_{m\ell}\mp\tilde{\theta}),R\sin(\theta_{m\ell}\mp\tilde{\theta}),c(\ell\mp1)],$$

$$\boldsymbol{R}_{A,m\pm1,\ell\mp2}=[R\cos(\theta_{m\ell}),R\sin(\theta_{m\ell}),c(\ell\mp2)],$$

$$\boldsymbol{R}_{A,m\pm1,\ell\mp1}=[R\cos(\theta_{m\ell}\pm\tilde{\theta}),R\sin(\theta_{m\ell}\pm\tilde{\theta}),c(\ell\mp1)], \tag{3}$$

where $\tilde{\theta}=\theta_1+\theta_2$. In fact, $\theta_{m\ell}$ is the angle seen by two adjacent A or two adjacent B carbon atoms along the circumference of the tube. At this point, it is useful to introduce unit vectors along the direction of carbon-carbon bonds: There are three unit vectors between atom A and its three nearest-neighbor B atoms, which are defined by $\boldsymbol{\delta}_i^1=[\boldsymbol{R}_{B,m\ell}^{(i)}-\boldsymbol{R}_{A,m\ell}]/a$, and six unit vectors between atom A and its six next-nearest-neighbor A atoms, which are defined by $\boldsymbol{\delta}_i^2=[\boldsymbol{R}_{A,m\ell}^{(i)}-\boldsymbol{R}_{A,m\ell}]/\sqrt{3}a$. Their explicit expressions can easily be calculated by using Eqs. (2) and (3) together with Eq. (1).

III. LATTICE VIBRATIONS

Lattice vibrations can be represented by the Hamiltonian

$$H_{lat}=\sum_j\frac{P_j^2}{2M}+\sum_{ij}[V_1(\boldsymbol{Q}_i,\boldsymbol{Q}_j)+V_2(\boldsymbol{Q}_i,\boldsymbol{Q}_j)]+\sum_{ijk}V_3(\boldsymbol{Q}_i,\boldsymbol{Q}_j,\boldsymbol{Q}_k), \tag{4}$$

where V_1 and V_2 are the interaction potentials between the first- and next-nearest-neighbor carbon atoms, respectively, and V_3 is the potential due to bond bending forces. It is necessary to consider, at least, the next-nearest-neighbor interactions in order to get a physical result, in particular, to obtain acoustical and flexure phonon modes.

In order to examine the ionic vibrations, we first define the displacements of the carbon atoms in three directions: these are in radial, tangential, and z directions on the tube. For a type A of carbon atom, they are denoted by $(Q_{A\rho},Q_{A\theta},Q_{Az})$, and on moving on the tube, it is necessary to include $j\equiv(m\ell)$ indices to label the other type A of carbon atoms; therefore,

$$Q_{A\beta,j}=\frac{1}{\sqrt{nN}}\sum_{\boldsymbol{q}}Q_{A\beta}(\boldsymbol{q})\exp[i(qc\ell+\alpha\theta_j)], \tag{5}$$

where $\boldsymbol{q}\equiv(q,\alpha)$ and β specify directions (ρ,θ,z). Here, while the wave vector q is used for the tube axis and is quasicontinuous for a finite tube, and as is previously noted, the other quantum number α takes $2n$ discrete values: $\alpha=0,\pm1,\pm2,\ldots,\pm(n-1),n$. The three nearest-neighbor atoms of $\boldsymbol{Q}_{A,m\ell}$ are $(\boldsymbol{Q}_{B,m\ell},\boldsymbol{Q}_{B,m-1,\ell+1},\boldsymbol{Q}_{B,m,\ell-1})$, in which each $\boldsymbol{Q}_{B,j}$ can be similarly expressed by

$$Q_{B\beta,j+\delta_i}=\frac{1}{\sqrt{nN}}\sum_{\boldsymbol{q}}Q_{B\beta}^{(i)}(\boldsymbol{q})\exp[i(qc\ell+\alpha\theta_j+\phi_i^0)], \tag{6}$$

with $i=1,2,3$. Here, it should be remembered that, as is indicated in the previous section, ϕ_i^0's are phase factors between atom A and its nearest-neighbor B-type carbon atoms, and with the help of the geometry given in Fig. 2, they are found as $\phi_1^0=\alpha\theta_1$, $\phi_2^0=-\alpha\theta_2+qc$, and $\phi_3^0=-\alpha\theta_2-qc$, respectively. In a similar way, the displacement of six next-nearest-neighbor atoms of A, $Q_{A\beta,j+\delta_i}$, can be written down as in Eq. (6), but with ϕ_i instead of ϕ_i^0. These are found as $\phi_1=\alpha\tilde{\theta}+qc$, $\phi_2=2qc$, $\phi_3=-\alpha\tilde{\theta}+qc$, $\phi_4=-\alpha\tilde{\theta}-qc$, $\phi_5=-2qc$, and $\phi_6=\alpha\tilde{\theta}-qc$.

A. Nearest- and next-nearest-neighbor interactions

By the above considerations, now, one is ready to calculate the potential energy V_1 for nearest-neighbor interactions,[16] $V_1=(K_1/2)\Sigma_{i,j}[\boldsymbol{\delta}_i^1\cdot(\boldsymbol{Q}_{B,j+\delta_i}-\boldsymbol{Q}_{A,j})]^2$, where K_1 is the spring constant that characterizes the central force along the bonds between carbon atoms. Before calculating V_1, for convenience, it is beneficial to rotate the coordinate system counterclockwise by an angle θ_j to a new one that transforms unit vectors of Cartesian coordinates $\tilde{\boldsymbol{x}}_i$'s to unit vectors of cylindrical coordinates $\tilde{\boldsymbol{e}}_i$'s by $\tilde{\mathbf{R}}_z$ with the symbolic matrix equation $\tilde{\boldsymbol{e}}_i=\tilde{\mathbf{R}}_z(\theta_j)\tilde{\boldsymbol{x}}_i$. Here, $\tilde{\mathbf{R}}_z$ is the rotation about the z axis and $\tilde{\boldsymbol{e}}_i^\dagger\equiv(\boldsymbol{\rho\theta z})$, $\tilde{\boldsymbol{x}}_i^\dagger\equiv(\boldsymbol{xyz})$ are the adjoints of 3×1 column matrices consisting of unit vectors of cylindrical and Cartesian coordinates, respectively. Therefore, it is now straightforward to express a typical member of displacements of A atoms in terms of transformation matrix elements as

$$\begin{aligned}&Q_{A\rho}(\boldsymbol{q})\boldsymbol{\rho}+Q_{A\theta}(\boldsymbol{q})\boldsymbol{\theta}+Q_{Az}(\boldsymbol{q})\boldsymbol{z}\\&\quad=Q_{A\rho}(\boldsymbol{q})(\cos\theta_{m\ell},\sin\theta_{m\ell},0)+Q_{A\theta}(\boldsymbol{q})\\&\quad\times(-\sin\theta_{m\ell},\cos\theta_{m\ell},0)+Q_{Az}(\boldsymbol{q})(0,0,1).\end{aligned} \tag{7}$$

Next, the same procedure can easily be applied to a member of nearest-neighbor B atoms, and hence the associated displacements would then be written as

$$\begin{aligned}&Q_{B\rho}^{(i)}(\boldsymbol{q})\boldsymbol{\rho}+Q_{B\theta}^{(i)}(\boldsymbol{q})\boldsymbol{\theta}+Q_{Bz}^{(i)}(\boldsymbol{q})\boldsymbol{z}\\&\quad=Q_{B\rho}^{(i)}(\boldsymbol{q})[\cos(\theta_{m\ell}+\theta_{\kappa_i}),\sin(\theta_{m\ell}+\theta_{\kappa_i}),0]\\&\quad+Q_{B\theta}^{(i)}(\boldsymbol{q})[-\sin(\theta_{m\ell}+\theta_{\kappa_i}),\cos(\theta_{m\ell}+\theta_{\kappa_i}),0]\\&\quad+Q_{Bz}^{(i)}(\boldsymbol{q})(0,0,1).\end{aligned} \tag{8}$$

θ_{κ_i} is defined to be θ_1 or $-\theta_2$ if the index i is equal to 1 or 2 and 3, respectively. Though it will be used in the remainder of this section, here is the place to give how the displacements of next-nearest-neighbor atoms of A, i.e., $\boldsymbol{Q}_A^{(i)}(\boldsymbol{q})$, can be written by using the same hierarchy. This can be achieved by taking $\theta_{m\ell}+\theta_{\kappa_i}$ instead of $\theta_{m\ell}$ in Eq. (7). However, here, θ_{κ_i} is assigned to be $\tilde{\theta}(0)$ when $i=1,6(2,5)$ and otherwise $-\tilde{\theta}$, i.e., for $i=3,4$. By taking into account this notation and using Eqs. (7) and (8) together with the related unit vectors in V_1, and similarly in V_2, the potential energy functionals for the nearest- and next-nearest-neighbor interactions become $V_k=(K_k/2)\Sigma_{j\equiv(m\ell)}\Sigma|\chi_{\mathbf{q},j}^{(i)k}|^2$, where

$$\chi_{\boldsymbol{q},j}^{(i)k}=\boldsymbol{\delta}_i^k\cdot(\boldsymbol{Q}_k^{(i)}-\boldsymbol{Q}_A)=e^{i(qc\ell+\alpha\theta_j)}\tilde{\chi}^{(i)k}, \tag{9}$$

with $k=1$ and 2. The explicit forms of all $\tilde{\chi}^{(i)k}$'s for both interactions[37] arising from Eq. (9) are given in Ref. 16. Now, it is possible to write down V_1 and V_2 in compact forms as $\mathbb{Q}^\dagger\mathbb{A}\mathbb{Q}$ with matrices defined by 6×1 column vector $\mathbb{Q}$ whose Hermitian conjugate is $\mathbb{Q}^\dagger=(Q_{A\rho}^*\ Q_{A\theta}^*\ Q_{Az}^*\ Q_{B\rho}^*\ Q_{B\theta}^*\ Q_{Bz}^*)$ and with $\mathbb{A}$ which is the square matrix of order 6: $V_1=(K_1/2)\Sigma_{i,j=1}^6\mathbb{Q}_i^\dagger\mathbb{A}_{ij}^{(1)}\mathbb{Q}_j$. After some algebra, matrix elements of $\mathbb{A}_{ij}^{(1)}$ can be easily obtained. Nonzero diagonal and nondiagonal matrix elements are presented in Appendix A explicitly by Eqs. (A1) and (A2), respectively. We can formally do the same thing for the next-nearest-neighbor interactions. In other words, the potential energy functional V_2 for the next-nearest-neighbor interactions has the similar form to V_1 but contains a different matrix $\mathbb{A}^{(2)}$ and spring constant K_2, instead of $\mathbb{A}^{(1)}$ and K_1, i.e., one has $V_2=(K_2/2)\Sigma_{i,j=1}^6\mathbb{Q}_i^\dagger\mathbb{A}_{ij}^{(2)}\mathbb{Q}_j$. Here, the superscripts 1 and 2 over $\mathbb{A}$ refer to the first- and second-nearest-neighbor interactions, respectively. The matrix $\mathbb{A}^{(2)}$ comes out to be in a block form of two (3×3) matrices, and its nonzero coefficients are also listed in Appendix A by Eq. (A3). We also notice that we have two types of next-nearest-neighbor interactions: One is between the atoms A-A and the second one between B-B, and each of them is included in a single (3×3) submatrix of $\mathbb{A}^{(2)}$.

B. Radial bond bending

Bonds between carbon atoms in the nanotube are bent in contradistinction to graphene sheets; therefore, it is necessary to consider bond bending in lattice vibration calculations in carbon nanotubes (CNTs). Within the nearest-neighbor interactions, if the unit vector between atoms A and B is $\boldsymbol{\delta}$, then the normal vector $\boldsymbol{n}$ in radial direction at the midpoint of the bond between A and B is defined by $\boldsymbol{n}=\boldsymbol{\delta}\times\boldsymbol{z}$. The potential energy functional due to bond bending is defined by[16] $V_3=(K_3/2)\Sigma_k|\Delta_k|^2$, in which $k=1,2$ refer to A and B, respectively, and $\Delta_{B(A)}$ is given by $\Delta_{B(A)}=\Sigma_{i=1}^3\boldsymbol{n}_i\cdot[\boldsymbol{Q}_{A(B)}^{(i)}-\boldsymbol{Q}_{B(A)}^{(0)}]$. Here, these two interactions are simplified as

$$\Delta_A=e^{i\alpha\theta_1}[D_1^*Q_{B\rho}-D_2^*Q_{B\theta}]-D_3Q_{A\rho},$$

$$\Delta_B=D_1Q_{A\rho}+D_2Q_{A\theta}-e^{i\alpha\theta_1}D_3Q_{B\rho}, \tag{10}$$

by means of new coefficients D_i whose explicit expressions are presented in Appendix A. Therefore, the potential energy functional due to bond bending can be written as $V_3=(K_3/2)\Sigma_{i,j=1}^6\mathbb{Q}_i^\dagger\mathbb{A}_{ij}^{(3)}\mathbb{Q}_j$, where the nonzero elements of $\mathbb{A}^{(3)}$ are also given in Appendix A by Eq. (A4). Consequently, the total potential energy functional becomes $V=(K_1/2)\Sigma_{i,j}\Sigma_{k=1}^3r_k\mathbb{Q}_i^\dagger\mathbb{A}_{ij}^{(k)}\mathbb{Q}_j$, where the last two interactions have been scaled according to $K_k=r_kK_1$. Finally, we can now write out the classical Hamiltonian for lattice vibrations as

$$H_{lat}=\frac{1}{2}M\sum_{\boldsymbol{q}\equiv(q,\alpha)}\sum_{i=1}^{6}\dot{\mathbb{Q}}_i^\dagger\dot{\mathbb{Q}}_i+\frac{1}{2}K_1\sum_{\boldsymbol{q}\equiv(q,\alpha)}\sum_{i,j}\sum_{k=1}^{3}r_k\mathbb{Q}_i^\dagger\mathbb{A}_{ij}^{(k)}\mathbb{Q}_j. \tag{11}$$

At this stage, it is useful to transform the coordinates to center of mass system so that quantization of lattice vibrations becomes easy to handle. These are defined as $Q_{A\beta}=Q_\beta+q_\beta/2$ and $Q_{B\beta}=Q_\beta-q_\beta/2$, where Q_β and q_β are the center of mass and relative coordinates, respectively, and β takes values of 1, 2, and 3 and refers to components (ρ,θ,z) of coordinates Q,q. It should be noted that this transformation is achieved concisely in matrix form by defining matrices

$$\mathbb{C}=\begin{pmatrix}\frac{1}{2}\end{pmatrix}\begin{pmatrix}2\mathbb{I} & \mathbb{I}\\ 2\mathbb{I} & -\mathbb{I}\end{pmatrix}$$

and

$$\mathbb{Q}^T=(Q_\rho\quad Q_\theta\quad Q_z\quad q_\rho\quad q_\theta\quad q_z)$$

with a (3×3) unit matrix $\mathbb{I}$. Therefore, introducing center of mass and relative coordinates corresponds to a coordinate transformation from $\bar{\mathbb{Q}}$ to $\mathbb{Q}$ accomplished by the matrix $\mathbb{C}$: $\mathbb{Q}=C\bar{\mathbb{Q}}$. As a result of this transformation, Eq. (11) becomes

$$H_{lat}=\frac{1}{2}M\sum_{\boldsymbol{q}\equiv(q,\alpha)}\dot{\bar{\mathbb{Q}}}^\dagger\mathbb{C}^\dagger\mathbb{C}\dot{\bar{\mathbb{Q}}}+\frac{1}{2}K_1\sum_{\boldsymbol{q}\equiv(q,\alpha)}\bar{\mathbb{Q}}^\dagger\mathbb{D}\bar{\mathbb{Q}}, \tag{12}$$

where $\mathbb{D}=\mathbb{C}^\dagger\bar{\mathbb{A}}\mathbb{C}=\Sigma_{k=1}^3r_k\mathbb{C}^\dagger\mathbb{A}^k\mathbb{C}$ has been used with $\bar{\mathbb{A}}_{ij}=\Sigma_{k=1}^3r_k\mathbb{A}_{ij}^k$. Here, since

$$\mathbb{C}^\dagger\mathbb{C}=\begin{pmatrix}2\mathbb{I} & 0\\ 0 & \mathbb{I}/2\end{pmatrix}=\begin{pmatrix}2 & 0\\ 0 & 0\end{pmatrix}\otimes\mathbb{I}+\mathbb{I}\otimes\begin{pmatrix}0 & 0\\ 0 & 1/2\end{pmatrix},$$

then the first term in Eq. (12), in fact, consists of the sum of kinetic energies of the terms with total mass $M_0=2M$ and with reduced mass $\mu_0=M/2$. The elements of the matrix $\mathbb{D}$ are defined as $\mathbb{D}_{ij}=\tilde{\mathbb{A}}_{ij}$ for $i(j)=1,2,3(1,2,3)$, $\mathbb{D}_{ij}=\tilde{\mathbb{A}}_{ij}/2$ for $i(j)=1,2,3(4,5,6)$ and $j(i)=4,5,6(1,2,3)$, and $\mathbb{D}_{ij}=\tilde{\mathbb{A}}_{ij}/4$ for $i(j)=4,5,6(4,5,6)$, wherein the elements $\tilde{\mathbb{A}}_{ij}$ can be expressed in terms of $\bar{\mathbb{A}}_{ij}$.

With these transformations and by introducing canonical momenta $\mathbb{P}^T=(P_\rho\ P_\theta\ P_z\ p_\rho\ p_\theta\ p_z)$ conjugate to $\bar{\mathbb{Q}}$, it is easy to show that Eq. (12) becomes

$$H_{lat}^{T}=\sum_{\boldsymbol{q}\equiv(q,\alpha)}\left[\frac{1}{2M_0}(|P_\rho|^2+|P_\theta|^2+|P_z|^2)+\frac{1}{2\mu_0}(|p_\rho|^2+|p_\theta|^2+|p_z|^2)\right]+\frac{1}{2}K_1\sum_{\boldsymbol{q}\equiv(q,\alpha)}\bar{\mathbb{Q}}^{\dagger}\mathbb{D}\bar{\mathbb{Q}}. \tag{13}$$

We note that all the concerned matrices are Hermitian.

C. Quantization of lattice waves

It is customary that the quantum mechanical investigation begins by introducing some creation and annihilation operators as follows:

$$Q_\beta^k(\boldsymbol{q})=\left[\frac{\hbar}{2M_k\omega_\beta(\boldsymbol{q})}\right]^{1/2}(a_{\boldsymbol{q}\beta}+a_{\boldsymbol{q}\beta}^{\dagger}),$$

$$P_\beta^k(\boldsymbol{q})=\frac{1}{i}\left[\frac{M_k\omega_\beta(\boldsymbol{q})\hbar}{2}\right]^{1/2}(a_{\boldsymbol{q}\beta}-a_{\boldsymbol{q}\beta}^{\dagger}),\quad \beta=1,2,3, \tag{14}$$

where $k(\beta)$ takes values 1 (1,2,3) and 2 (4,5,6), and they refer to center of mass and relative coordinates and momenta, respectively. In other words, $Q_\beta^k(P_\beta^k)$ and M_k are reduced to $Q_\beta(P_\beta)$ and $q_\beta(p_\beta)$ and total and reduced masses, i.e., M_0 and μ_0, respectively. In Eqs. (14), $a_{\boldsymbol{q}\beta}(a_{\boldsymbol{q}\beta}^{\dagger})$ defines annihilation (creation) operators for the center of mass and relative motions $\beta=1,2,3$ and $\beta=4,5,6$, separately; furthermore, $\omega_\beta(\boldsymbol{q})$ is introduced here as a dummy frequency and will disappear in a natural way during the diagonalization procedure. If we substitute Eqs. (14) into Eq. (13) and use the index i instead of β, then the Hamiltonian becomes

$$H_{ph}=\sum_{\boldsymbol{q}\equiv(q,\alpha)}\sum_{i=1}^{6}\left[\hbar\omega_i^{+}(\boldsymbol{q})(a_{\boldsymbol{q}i}^{\dagger}a_{\boldsymbol{q}i}+a_{\boldsymbol{q}i}a_{\boldsymbol{q}i}^{\dagger})+\hbar\omega_i^{-}(\boldsymbol{q})(a_{\boldsymbol{q}i}^{2}+a_{\boldsymbol{q}i}^{\dagger 2})+\frac{1}{2}\sum_{j(\neq i)}\hbar\omega_{ij}(\boldsymbol{q})(a_{\boldsymbol{q}i}a_{\boldsymbol{q}j}^{\dagger}+a_{\boldsymbol{q}i}a_{\boldsymbol{q}j}+\text{H.c.})\right], \tag{15}$$

where the frequencies are defined by the following relations:

$$\omega_i^{\mp}(\boldsymbol{q})=\frac{1}{4}\left[\mp\omega_i(\boldsymbol{q})+\frac{K_1}{2M}\frac{\tilde{\mathbb{A}}_{ii}}{\omega_i(\boldsymbol{q})}\right],$$

$$\omega_{ij}(\boldsymbol{q})=\frac{K_1}{8M}\frac{\tilde{\mathbb{A}}_{ij}+\tilde{\mathbb{A}}_{ij}^{*}}{[\omega_i(\boldsymbol{q})\omega_j(\boldsymbol{q})]^{1/2}}, \tag{16}$$

where $\tilde{\mathbb{A}}_{ij}$'s have the property $\tilde{\mathbb{A}}_{ij}^{*}=\tilde{\mathbb{A}}_{ji}$, and their diagonal components together with nondiagonal ones different from zero are all presented in Appendix A by Eqs. (A5) and (A6). It appears that the first term in the above Hamiltonian is already diagonalized, while the second and third terms contain bilinear operators; furthermore, the last term comprises a mixture of center of mass and relative modes. It is possible to calculate the contribution from bilinear terms of operators to the energy by introducing canonical transformations, as achieved in large polaron theory, where application of the squeezed state transformations makes the bilinear terms diagonalize and also generates squeezed phonon states.[38] In general, the unitary transformation method is thoroughly investigated in condensed matter physics by Wagner,[39] and in the present work, we use relevant transformations of this reference widely.

D. Diagonalization

1. First diagonalization

In order to diagonalize the second term of Eq. (15), it is necessary to make a canonical transformation by a unitary operator $U_1=\exp[S_1(\boldsymbol{q})]$, with $S_1(\boldsymbol{q})=\Sigma_k\lambda_k(a_{\boldsymbol{q}k}^{2}-a_{\boldsymbol{q}k}^{\dagger 2})/2$, under which the operator $a_{\boldsymbol{q}i}$ transforms as $\tilde{a}_{\boldsymbol{q}i}=a_{\boldsymbol{q}i}\cosh\lambda_i-a_{\boldsymbol{q}i}^{\dagger}\sinh\lambda_i$. Hence, the transformed Hamiltonian becomes $\tilde{H}_{ph}=\Sigma_{\boldsymbol{q}}\Sigma_{i=1}^{6}(\tilde{H}_i+\tilde{H}_{ij})$, with

$$\tilde{H}_i=[\hbar\omega_i^{+}(\boldsymbol{q})\cosh 2\lambda_i-\hbar\omega_i^{-}(\boldsymbol{q})\sinh 2\lambda_i](a_{\boldsymbol{q}i}^{\dagger}a_{\boldsymbol{q}i}+a_{\boldsymbol{q}i}a_{\boldsymbol{q}i}^{\dagger})+[\hbar\omega_i^{-}(\boldsymbol{q})\cosh 2\lambda_i-\hbar\omega_i^{+}(\boldsymbol{q})\sinh 2\lambda_i](a_{\boldsymbol{q}i}^{2}+a_{\boldsymbol{q}i}^{\dagger 2}) \tag{17}$$

and

$$\tilde{H}_{ij}=\frac{1}{2}\sum_{j(\neq i)}\hbar\omega_{ij}(\boldsymbol{q})\exp[-(\lambda_i+\lambda_j)](a_{\boldsymbol{q}i}a_{\boldsymbol{q}j}^{\dagger}+a_{\boldsymbol{q}i}a_{\boldsymbol{q}j}+\text{H.c.}). \tag{18}$$

If $\tanh 2\lambda_i=\omega_i^{-}/\omega_i^{+}$, then the second term of $\tilde{H}_i$ vanishes, and hence it is diagonalized with a new frequency but $\tilde{H}_{ij}$ is still in a nondiagonal form. It should be pointed out that the variation of the expectation value of $\tilde{H}_i$ by phonon vacuum, i.e., $\langle\tilde{H}_i\rangle_0$, with respect to λ_i gives the same condition for diagonalization, i.e., $\tanh 2\lambda_i=\omega_i^{-}/\omega_i^{+}$. Since its solution yields $\sinh 2\lambda_i=\omega_i^{-}/[\omega_i^{+2}(\boldsymbol{q})-\omega_i^{-2}(\boldsymbol{q})]^{1/2}$ and $\cosh 2\lambda_i=\omega_i^{+}/[\omega_i^{+2}(\boldsymbol{q})-\omega_i^{-2}(\boldsymbol{q})]^{1/2}$, after the first transformation, the phonon Hamiltonian becomes

$$\tilde{H}_{ph}=\frac{1}{2}\sum_{\boldsymbol{q}\equiv(q,\alpha)}\sum_{i=1}^{6}\left[\hbar\omega_i^{(0)}(\boldsymbol{q})(a_{\boldsymbol{q}i}^{\dagger}a_{\boldsymbol{q}i}+a_{\boldsymbol{q}i}a_{\boldsymbol{q}i}^{\dagger})+\sum_{j(\neq i)}\hbar\omega_{ij}^{(0)}(\boldsymbol{q})(a_{\boldsymbol{q}i}^{\dagger}a_{\boldsymbol{q}j}+a_{\boldsymbol{q}i}^{\dagger}a_{\boldsymbol{q}j}^{\dagger}+\text{H.c.})\right], \tag{19}$$

where $\omega_i^{(0)}(\boldsymbol{q})=(K_1\tilde{\mathbb{A}}_{ii}/2M)^{1/2}$ and $\omega_{ij}^{(0)}(\boldsymbol{q})=(K_1/2M)^{1/2}(\tilde{\mathbb{A}}_{ij}+\tilde{\mathbb{A}}_{ij}^{*})/[4(\tilde{\mathbb{A}}_{ii}\tilde{\mathbb{A}}_{jj})^{1/4}]$. It should be noticed that the new renormalized frequencies $\omega_i^{(0)}(\boldsymbol{q})$ and $\omega_{ij}^{(0)}(\boldsymbol{q})$ do not contain the dummy frequency $\omega_i(\boldsymbol{q})$ chosen for the quantization procedure of Eqs. (14). When we calculate $\omega_i^{(0)}(\boldsymbol{q})$, we see that, for $\alpha=0$, it gives good results for certain optical phonon frequencies such as 170, 865, 1596, and 1600 cm^{-1} at the Γ point of the Brillouin zone, but for the $q\neq 0$ points, the diagonal part is far from giving a satisfactory result for the phonon spectra (see Fig. 3); therefore one has to consider contribution from the new nonlinear terms which requires further diagonalization.

It is useful to express the above Hamiltonian in dimensionless form by using a typical phonon frequency. If we

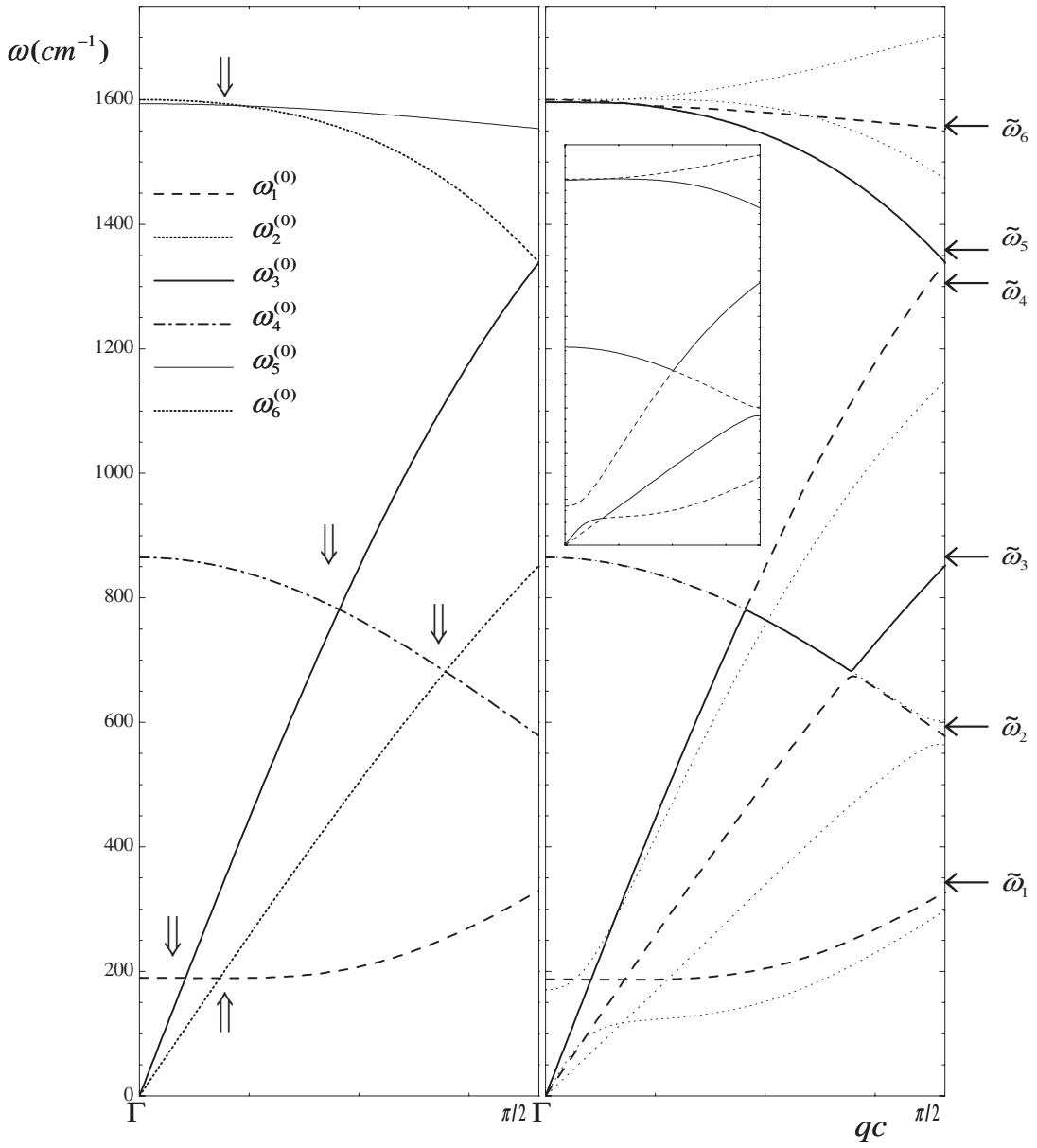

FIG. 3. For $\alpha=0$, q dependence of the phonon spectra according to Eq. (20) (left panel). In the right panel, again q dependence of the phonon spectra, but after the second unitary transformation, according to Eq. (33), together with their comparison with those found by Mahan and Jeon [the solid and dashed lines correspond to the results of Eq. (33), and the dotted lines to those of Ref. 16]. To make the comparison easy, the results of Ref. 16 are also given in the inset.

define a frequency ω_0 by the relation $K_1/M=\omega_0^2/3$, then this gives the well-known Raman line, which is $\omega_0=1600\ \mathrm{cm}^{-1}$. Hence, dimensionless energy and frequencies will be scaled as $\bar{H}=\tilde{H}/\hbar\omega_0$, $\bar{\omega}_i^{(0)}(\boldsymbol{q})=\omega_i^{(0)}(\boldsymbol{q})/\omega_0$, and $\bar{\omega}_{ij}^{(0)}(\boldsymbol{q})=\omega_{ij}^{(0)}(\boldsymbol{q})/\omega_0$, such that $\omega_i^{(0)}(\boldsymbol{q})$ and $\omega_{ij}^{(0)}(\boldsymbol{q})$ in Eq. (19) become

$$\bar{\omega}_i^{(0)}(\boldsymbol{q})=\left(\frac{\tilde{\mathbb{A}}_{ii}}{6}\right)^{1/2},\quad \bar{\omega}_{ij}^{(0)}(\boldsymbol{q})=\frac{1}{2\sqrt{6}}\frac{\mathrm{Re}\ \tilde{\mathbb{A}}_{ij}}{(\tilde{\mathbb{A}}_{ii}\tilde{\mathbb{A}}_{jj})^{1/4}}. \quad (20)$$

2. Second diagonalization

After each transformation, the new Hamiltonian contains the same amount of bilinear terms as the original one, but frequencies have become renormalized so that they approach the correct results. In order to get accurate results it appears that one needs to employ a number of consecutive transformations. In the present problem, this approach does not give results as accurate as one expects after several transformations. However, instead of applying many transformations, we can make use of one with a slight improvement of its application on the physical basis.

Instead of considering six components of Eq. (19) altogether, it is advantageous to focus on a single component and utilize a transformation that will diagonalize it in a way that includes the correlation of this particular component with the others. First, we choose the component i of the Hamiltonian given by Eq. (19),

$$\bar{H}_i = \frac{1}{2}\sum_{\boldsymbol{q}\equiv(q,\alpha)}\Bigg[\bar{\omega}_i^{(0)}(\boldsymbol{q})(a_{\boldsymbol{q}i}^\dagger a_{\boldsymbol{q}i} + a_{\boldsymbol{q}i}a_{\boldsymbol{q}i}^\dagger) + \sum_{j(\neq i)}\bar{\omega}_j^{(0)}(\boldsymbol{q})(a_{\boldsymbol{q}j}^\dagger a_{\boldsymbol{q}j} + a_{\boldsymbol{q}j}a_{\boldsymbol{q}j}^\dagger)\Bigg] + \frac{1}{2}\sum_{\boldsymbol{q}\equiv(q,\alpha)}\sum_{j(\neq i)}\Bigg[\bar{\omega}_{ij}^{(0)}(\boldsymbol{q})(a_{\boldsymbol{q}i}^\dagger a_{\boldsymbol{q}j} + a_{\boldsymbol{q}i}^\dagger a_{\boldsymbol{q}j}^\dagger + \text{H.c.}) + \sum_{k\neq j}\bar{\omega}_{jk}^{(0)}(\boldsymbol{q})(a_{\boldsymbol{q}j}^\dagger a_{\boldsymbol{q}k} + a_{\boldsymbol{q}j}^\dagger a_{\boldsymbol{q}k}^\dagger + \text{H.c.})\Bigg], \tag{21}$$

where the first term is already diagonal while the second one is not since we consider the ith component, and the third term represents the interactions between ith and the other five components. The fourth term appears to represent the interactions between the five components, but it includes implicitly the effect of the chosen ith component. The last two are nonlinear terms and will be neglected in the diagonalization procedure. Except the last two terms, the contributions of the other components to the ith frequency of the first term can be achieved by a second transformation defined by[39] $U_2=\exp[S_2(\boldsymbol{q})]$, with $S_2(\boldsymbol{q})=\Sigma_{j\neq i}\lambda_j(a_{\boldsymbol{q}i}a_{\boldsymbol{q}j}^\dagger - a_{\boldsymbol{q}i}^\dagger a_{\boldsymbol{q}j})$. Under this unitary operator, $a_{\boldsymbol{q}i}$ and $a_{\boldsymbol{q}j}$ transform as

$$\tilde{a}_{\boldsymbol{q}i} = a_{\boldsymbol{q}i}\cos\Lambda - \sum_j \bar{\lambda}_j(\sin\Lambda)a_{\boldsymbol{q}j}, \tag{22}$$

$$\tilde{a}_{\boldsymbol{q}j} = a_{\boldsymbol{q}i}\bar{\lambda}_j\sin\Lambda + \sum_k a_{\boldsymbol{q}k}[\delta_{jk} - (1-\cos\Lambda)\bar{\lambda}_j\bar{\lambda}_k], \tag{23}$$

where $\Lambda^2=\Sigma_{i\neq j}\lambda_j^2$ or $1=\Sigma_{i\neq j}\bar{\lambda}_j^2$ is the normalization condition for the transformation parameter. It should be noted that, though we use the same symbol for the transformation parameter as in U_1, they are physically different quantities. Furthermore, we also note that $\tilde{a}_{\boldsymbol{q}i}$ and $\tilde{a}_{\boldsymbol{q}j}^\dagger$ commute: $[\tilde{a}_{\boldsymbol{q}i},\tilde{a}_{\boldsymbol{q}j}^\dagger]=0$. Hence, the final transformed Hamiltonian $\bar{H}_i' = U_2^\dagger \bar{H}_i U_2$ contains, apart from diagonalized operators $(a_{\boldsymbol{q}i}a_{\boldsymbol{q}i}^\dagger + a_{\boldsymbol{q}i}^\dagger a_{\boldsymbol{q}i})$, nondiagonal operators such as $a_{\boldsymbol{q}i}^\dagger a_{\boldsymbol{q}j}$, $a_{\boldsymbol{q}i}a_{\boldsymbol{q}j}^\dagger$, $a_{\boldsymbol{q}j}^2$, $a_{\boldsymbol{q}i}a_{\boldsymbol{q}j}$,…, whose coefficients now comprise $\sin\Lambda$, $\cos\Lambda$, $\omega_i^{(0)}(\boldsymbol{q})$, and $\omega_{ij}^{(0)}(\boldsymbol{q})$:

$$\bar{H}_i' = \frac{1}{2}\sum_{\boldsymbol{q}\equiv(q,\alpha)}\Bigg[\tilde{\omega}_i(a_{\boldsymbol{q}i}^\dagger a_{\boldsymbol{q}i} + a_{\boldsymbol{q}i}a_{\boldsymbol{q}i}^\dagger) + \tilde{\omega}_i^+(a_{\boldsymbol{q}i}^{\dagger 2} + a_{\boldsymbol{q}i}^2) + \sum_{j\neq i}\tilde{\omega}_j(a_{\boldsymbol{q}j}^\dagger a_{\boldsymbol{q}j} + a_{\boldsymbol{q}j}a_{\boldsymbol{q}j}^\dagger) + \sum_{j\neq i}\tilde{\omega}_{ij}(a_{\boldsymbol{q}i}^\dagger a_{\boldsymbol{q}j} + a_{\boldsymbol{q}i}a_{\boldsymbol{q}j}^\dagger) + \sum_{j(\neq i)}\tilde{\omega}_{ij}^+(a_{\boldsymbol{q}i}^\dagger a_{\boldsymbol{q}j}^\dagger + a_{\boldsymbol{q}i}a_{\boldsymbol{q}j}) + \sum_{j(\neq i)}\sum_{k\neq j}\tilde{\omega}_{jk}(a_{\boldsymbol{q}j}^\dagger a_{\boldsymbol{q}k} + a_{\boldsymbol{q}j}a_{\boldsymbol{q}k}^\dagger) + \sum_{j(\neq i)}\sum_{k\neq j}\tilde{\omega}_{jk}^+(a_{\boldsymbol{q}j}^\dagger a_{\boldsymbol{q}k}^\dagger + a_{\boldsymbol{q}j}a_{\boldsymbol{q}k})\Bigg], \tag{24}$$

where the coefficients $\tilde{\omega}$ can be easily found after some algebra. Here, we present only the diagonal one, $\tilde{\omega}_i$, i.e.,

$$\tilde{\omega}_i = \bar{\omega}_i^{(0)}\cos^2\Lambda + \sum_{j(\neq i)}\Bigg[\bar{\omega}_j^{(0)}\bar{\lambda}_j^2\sin^2\Lambda + \bar{\omega}_{ij}^{(0)}\bar{\lambda}_j\sin\Lambda\cos\Lambda + \sum_{k\neq j}\bar{\omega}_{jk}^{(0)}\bar{\lambda}_j\bar{\lambda}_k\sin^2\Lambda\Bigg].$$

Here, we note that the ith component is coupled with the other five through $\tilde{\omega}_{ij}$ and $\tilde{\omega}_{ij}^+$. If we leave out the nonlinear terms, it is necessary that $\tilde{\omega}_{ij}$ should disappear for a full decoupling. If we now equate the coefficient $\tilde{\omega}_{ij}$ to zero, which also corresponds to minimization of the energy with respect to $\bar{\lambda}_j$, then we obtain

$$\tan 2\Lambda = \frac{\Gamma}{\bar{\omega}_i^{(0)} - \Pi - L}, \tag{25}$$

$$\bar{\lambda}_j = -\frac{\Delta_j + [\bar{\omega}_{ij}^{(0)}(\cot\Lambda)/2]}{\bar{\omega}_j^{(0)} - (\Pi + L) - [\Gamma(\cot\Lambda)/2]}, \tag{26}$$

wherein the new abbreviations are introduced as follows: $\Gamma = \Sigma_{k\neq i}\bar{\omega}_{ik}^{(0)}(\boldsymbol{q})\bar{\lambda}_k$, $\Pi=\Sigma_{k\neq i}\bar{\omega}_k^{(0)}(\boldsymbol{q})\bar{\lambda}_k^2$, $\Delta_j=\Sigma_{k\neq i}\bar{\omega}_{kj}^{(0)}(\boldsymbol{q})\bar{\lambda}_k$, and $L=\Sigma_j\Sigma_{k\neq i}\bar{\omega}_{kj}^{(0)}(\boldsymbol{q})\bar{\lambda}_k\bar{\lambda}_j$. Substitution of $\bar{\lambda}_j$ and Λ given by Eqs. (25) and (26), respectively, into $\tilde{\omega}_i$ yields a new frequency we look for $\tilde{\omega}_i=[(\bar{\omega}_i^{(0)}+\Pi+L)+\sqrt{(\bar{\omega}_i^{(0)}-\Pi-L)^2+\Gamma^2}]/2$. If the above requirement is fulfilled, then $\tilde{\omega}_i$ will become an eigenvalue of the transformed Hamiltonian. In order to improve this approach further, it is now advantageous to work with the Hamiltonian in the projective form.

3. Resolvent formalism

Instead of creation and annihilation operators, the same Hamiltonian with the relevant bilinear parts can be expressed in terms of state vectors, and therefore the corresponding Schrödinger equation becomes $\left[\bar{H}_{0i}' - \frac{1}{2}\tilde{\omega}_i(\boldsymbol{q})\right]|\varphi_i\rangle = -V|\varphi_i\rangle$, where

$$\bar{H}_{0i}' = \frac{1}{2}\sum_{\boldsymbol{q}}\Bigg[\tilde{\omega}_i(\boldsymbol{q})(2\Lambda_i+1) + \sum_{j\neq i}\tilde{\omega}_j(\boldsymbol{q})(2\Lambda_j+1)\Bigg],$$

$$V = \frac{1}{2}\sum_{\boldsymbol{q}}\Bigg[\sum_{j\neq i}\tilde{\omega}_{ij}(\boldsymbol{q})(\Lambda_{ij}+\Lambda_{ji}) + \sum_{j(\neq i)}\sum_{k\neq j}\tilde{\omega}_{jk}(\Lambda_{jk}+\Lambda_{kj})\Bigg],$$

with the projection operator $\Lambda_{ij}=|\varphi_i\rangle\langle\varphi_j|$. The phonon states $|\varphi_i\rangle$ are defined by the relation $[\bar{H}_i' - \tilde{\omega}_i(\boldsymbol{q})/2]|\varphi_i\rangle = 0$. The solution to such an equation can be obtained by using resolvent formalism as discussed in Ref. 39. We can then multiply the corresponding Schrödinger equation by its resolvent or Green's function $[\bar{H}_{0i}' - \tilde{\omega}_i(\boldsymbol{q})/2]^{-1}$,

$$\frac{1}{\left(\bar{H}_{0i}' - \frac{1}{2}\tilde{\omega}_i(\boldsymbol{q})\right)} = \frac{1}{\bar{\omega}_i^{(0)}(\boldsymbol{q}) - \tilde{\omega}_i(\boldsymbol{q})}(2\Lambda_i+1) + \sum_{j\neq i}\frac{1}{\bar{\omega}_j^{(0)}(\boldsymbol{q}) - \tilde{\omega}_i(\boldsymbol{q})}(2\Lambda_j+1), \tag{27}$$

to yield

$$|\varphi_i\rangle = -\frac{1}{\bar{\omega}_i^{(0)}(\boldsymbol{q}) - \tilde{\omega}_i(\boldsymbol{q})}\sum_{j\neq i}\frac{\bar{\omega}_{ij}^{(0)}(\boldsymbol{q})}{2}\Lambda_{ij}|\varphi_i\rangle - \sum_{j\neq i}\frac{[\bar{\omega}_{ij}^{(0)}(\boldsymbol{q})/2]}{\bar{\omega}_j^{(0)}(\boldsymbol{q}) - \tilde{\omega}_i(\boldsymbol{q})}\Lambda_{ji}|\varphi_i\rangle - \sum_{j(\neq i)}\sum_{k\neq j}\frac{[\bar{\omega}_{jk}^{(0)}(\boldsymbol{q})/2]}{\bar{\omega}_j^{(0)}(\boldsymbol{q}) - \tilde{\omega}_i(\boldsymbol{q})}\Lambda_{jk}|\varphi_i\rangle. \tag{28}$$

The multiplication of the last equation by $\langle\varphi_i|$ and $\langle\varphi_j|$, in turn, on the left provides two equations, and then we obtain the following two statements on comparing their coefficients:

$$\cos\Lambda = -\frac{1}{\bar{\omega}_i^{(0)}(\boldsymbol{q}) - \tilde{\omega}_i(\boldsymbol{q})}\frac{\Gamma}{2}\sin\Lambda, \tag{29}$$

$$\bar{\lambda}_j \sin\Lambda = -\frac{1}{\bar{\omega}_j^{(0)}(\boldsymbol{q}) - \tilde{\omega}_i(\boldsymbol{q})}\left[\frac{1}{2}\tilde{\omega}_{ij}^{(0)}\cos\Lambda + \Delta_j \sin\Lambda\right], \tag{30}$$

which can be utilized to eliminate Λ, Γ, and Δ_j to obtain the frequency $\tilde{\omega}_i(\boldsymbol{q})$ of the ith component that we are concerned with. It should be pointed out that all the components specified so far by the indices running from 1 to 6 represent the center of mass and relative coordinates and in reality, after quantization, they qualify phonon modes, and considering the matrix elements $\tilde{\mathbb{A}}_{ij}$ that contain the quantum numbers α along the circumference direction of the nanotube, they determine the correct number of modes of the phonon spectra.

In order to simplify the calculation further, we make an *ad hoc* assumption about the couplings between the components in such a way that while the diagonalization of the particular state is complete, say i, the residual nondiagonality among the other components is to be minimal. This is well known as the Fano problem.[40] Let us first consider the diagonalization of the distinguished component i itself, i.e., take $\Delta_j=0$, which corresponds to the case where $|\varphi_i\rangle$ is coupled to all the others, whereas the others are not mutually coupled; this results in the relation

$$\tilde{\omega}_i(\boldsymbol{q}) - \bar{\omega}_i^{(0)}(\boldsymbol{q}) = \sum_{j\neq i}^{6}\frac{1}{\tilde{\omega}_i(\boldsymbol{q}) - \bar{\omega}_j^{(0)}(\boldsymbol{q})}\left[\frac{\bar{\omega}_{ij}^{(0)}(\boldsymbol{q})}{2}\right]^2, \tag{31}$$

from which the $\tilde{\omega}_i(\boldsymbol{q})$ frequencies are to be calculated. We note that some terms, such as $\bar{\omega}_{12}^{(0)}$, $\bar{\omega}_{13}^{(0)}$, $\bar{\omega}_{14}^{(0)}$, $\bar{\omega}_{25}^{(0)}$, $\bar{\omega}_{26}^{(0)}$, $\bar{\omega}_{35}^{(0)}$, $\bar{\omega}_{36}^{(0)}$, $\bar{\omega}_{45}^{(0)}$, and $\bar{\omega}_{46}^{(0)}$, vanish, which arises from the fact that the relevant matrix elements $\tilde{\mathbb{A}}_{ij}$ are pure imaginary. Therefore, some terms on the right-hand side of the above equation are missing, and eventually one gets a cubic algebraic equation, $\tilde{\omega}_i^3 + \tilde{\Omega}_{(ijk)}^{(2)}\tilde{\omega}_i^2 + \tilde{\Omega}_{(ijk)}^{(1)}\tilde{\omega}_i + \tilde{\Omega}_{(ijk)}^{(0)} = 0$, whose three distinct real roots are

$$\tilde{\omega}_i(\boldsymbol{q}) = -\frac{1}{3}\tilde{\Omega}_{(ijk)}^{(2)} + \frac{2}{3}\tilde{\Omega}_{(ijk)}^{(+)} \times \begin{cases} \pm\cos\frac{1}{3}[\arccos(\mp\tilde{\Omega}_{(ijk)}^{(-)}/2[\tilde{\Omega}_{(ijk)}^{(+)}]^3)] \\ -\cos\left\{\frac{1}{3}[\arccos(-\tilde{\Omega}_{(ijk)}^{(-)}/2[\tilde{\Omega}_{(ijk)}^{(+)}]^3)] + \frac{\pi}{3}\right\}. \end{cases} \tag{32}$$

Instead of well-known Cardan's algebraic solutions to the cubic equation,[41] we have used their trigonometric equivalents[42] due to their compactness. In Eq. (32), we have defined the following quantities:

$$\tilde{\Omega}_{(ijk)}^{(2)} = -[\bar{\omega}_i^{(0)} + \bar{\omega}_j^{(0)} + \bar{\omega}_k^{(0)}],$$

$$\tilde{\Omega}_{(ijk)}^{(1)} = \bar{\omega}_i^{(0)}\bar{\omega}_j^{(0)} + \bar{\omega}_i^{(0)}\bar{\omega}_k^{(0)} + \bar{\omega}_k^{(0)}\bar{\omega}_j^{(0)} - \frac{1}{4}[(\bar{\omega}_{ij}^{(0)})^2 + (\bar{\omega}_{ik}^{(0)})^2],$$

$$\tilde{\Omega}_{(ijk)}^{(0)} = \frac{1}{4}[\bar{\omega}_k^{(0)}(\bar{\omega}_{ij}^{(0)})^2 + \bar{\omega}_j^{(0)}(\bar{\omega}_{ik}^{(0)})^2] - \bar{\omega}_i^{(0)}\bar{\omega}_j^{(0)}\bar{\omega}_k^{(0)},$$

and used the abbreviations $\tilde{\Omega}_{(ijk)}^{(+)} = \{[\tilde{\Omega}_{(ijk)}^{(2)}]^2 - 3\tilde{\Omega}_{(ijk)}^{(1)}\}^{1/2}$ and $\tilde{\Omega}_{(ijk)}^{(-)} = \{27\tilde{\Omega}_{(ijk)}^{(0)} + 2[\tilde{\Omega}_{(ijk)}^{(2)}]^3 - 9\tilde{\Omega}_{(ijk)}^{(1)}\tilde{\Omega}_{(ijk)}^{(2)}\}$. All roots obtained turn out to be real since $\tilde{\Omega}_{(ijk)}^{(-)}/2[\tilde{\Omega}_{(ijk)}^{(+)}]^3 < -1$ is satisfied in every case and therefore it represents the irreducible case where all the roots are real. When one needs to include the correlation effect between the other components, by taking into account $\Delta_j \neq 0$, diagonalization of other states with $\Delta_j \neq 0$ is needed. This, at a first glance, seems to be more complicated, but one reaches the same result as Eq. (31) when $\Delta_j \neq 0$ is taken into account i.e., Eq. (31) can be used for other five states.[39] Equation (31) for six different i's yields six cubic equations in $\tilde{\omega}_i(\boldsymbol{q})$ resulting with 18 roots. Nevertheless, having known that the roots having the lowest symmetry are eligible, the remaining task is to look for a way of classifying them according to this rule. Solutions satisfying these rules which come from the cubic ones have the form

$$\tilde{\omega}_i(\boldsymbol{q}) = -\frac{1}{3}\tilde{\Omega}_{(ijk)}^{(2)} + \frac{2}{3}\tilde{\Omega}_{(ijk)}^{(+)}\cos\frac{1}{3}\tilde{\Omega}_{(ijk)}, \tag{33}$$

where

$$\tilde{\Omega}_{(ijk)} = \arccos(-\tilde{\Omega}_{(ijk)}^{(-)}/2[\tilde{\Omega}_{(ijk)}^{(+)}]^3) + 2\pi k_i.$$

k_i takes values 1, 0, and 2 when i is equal to 1 (or 2), 4 (or 6), and 3 (or 5), respectively. In this respect, it should be noted that, for $i=1,\ldots,6$, allowed values of j and k which we show here by a (jk) pair for shorthand notation are (56), (34), (24), (23), (16), and (15), respectively. These are the phonon frequencies corresponding to each quantum number α.

E. Results

After the canonical transformations and the resolvent formalism, we have obtained the phonon Hamiltonian in the dimensionless and diagonalized form as $\bar{H}_{ph} = \Sigma_{\boldsymbol{q}\equiv(q,\alpha)}\Sigma_{i=1}^{6}\tilde{\omega}_i(\boldsymbol{q})(a_i^\dagger a_i + a_i a_i^\dagger)$, where we now have the phonon frequencies $\tilde{\omega}_i$ in an analytical form. For a (n,n)-armchair carbon nanotube, there are $N=2n$ carbon atoms in a unit cell; hence, the total number of phonon branches is $6N$. In order to characterize the phonon modes, one needs to know the symmetry of armchair carbon nanotubes, which is described by nonsymmorphic rod groups (or line groups). Full symmetry of the line groups is investigated in a series of papers by Damnjanović *et al.*[17,43,44] The (n,n)-armchair carbon nanotubes with either even or odd index n have a rod group $\mathcal{G}[n]$, whose point group $\mathcal{G}_0[n]$ is isomorphic to $\mathcal{D}_{2nh}$, and their irreducible representations at the Γ point are carefully analyzed by Alon in a recent work,[25] where also correct number of Raman and IR active modes are determined. The $6N$ phonon modes transform according to the irreducible representations of $\mathcal{D}_{2nh}$ and of these modes,

eight Raman-active transform as $\Gamma_R = 2A_{1g} \oplus 2E_{1g} \oplus 4E_{2g}$, and three infrared-active transform as $\Gamma_{IR} = 3E_{1u}$ and are fixed for all armchair nanotubes. These results are endorsed by experimental data.[45,46]

At this point, we choose specific chiral numbers for a sample armchair nanotube as (10, 10), since there are numerous works with which we compare the present results. There are 66 distinct branches in the phonon spectra, corresponding to 120 vibrational degrees of freedom in a unit cell of the nanotube, of which 12 modes are nondegenerate and 54 are doubly degenerate. We take the three scaling factors for force-constant parameters as $r_1 = 1.000$, $r_2 = 0.060$, and $r_3 = 0.024$ as in the work of Mahan and Jeon, Ref. 16. It appears that the final results for the phonon frequencies are very sensitive to small changes in these parameters.

For a quantitative analysis of the present approach, we compute the phonon modes for $\alpha = 0$ with the expression $\omega_i^{(0)}$ obtained after the first transformation. Figure 3 shows the six nondegenerate modes, of which the two are acoustical and the four are optical whose values at the Γ point coincide with the results of Mahan and Jeon, Ref. 16, as seen in Fig. 3. However, as one increases the wave vector q, discrepancies appear in the spectra, which necessitate a further diagonalization. Apart from the disagreement for $q \neq 0$, there is a major drawback of the results arising from the disregard of nondiagonal terms, that is, it does not accommodate mode mixing where acoustical and optical modes combine to remove degeneracies at the crossing points. In order to remedy this, we have performed a second transformation to diagonalize certain nonlinear terms and immediately after that, the correct dispersion relations have been obtained analytically within the scheme of the Fano problem, in spite of neglecting some nonlinear terms. In Fig. 3, we see that inclusion of the nonlinear terms indeed removes some degeneracies and bring forward mode mixing so that a partial agreement with results of Mahan and Jeon is obtained. However, as seen from Fig. 4, both mode crossings and mixings at low energies, in particular, involving acoustical modes, show the same behaviors as in various works, Refs. 11, 12, 15, and 23.

Essentially, by the first transformation, we have calculated contributions coming from the terms a_{qi}^2 and $(a_{qi}^\dagger)^2$ to the frequency of mode i. In the second transformation, we have considered modifications due to the terms such as $a_{qj}^\dagger a_{qj}$, $a_{qi}^\dagger a_{qj}$, and $a_{qj}^\dagger a_{qk}$ and their conjugates for $i \neq j \neq k$ to $\omega_i^{(0)}$, during which we have left out $a_{qi}^\dagger a_{qj}^\dagger$, $a_{qj}^\dagger a_{qk}^\dagger$, and their conjugates for $i \neq j \neq k$. We ascribe the mode mixing to inclusion of these nonlinear terms and the Fano procedure expedite to choose the correct roots analytically.

We note that for $\alpha = 0$, there are six nondegenerate modes, of which two are acoustical and the rest are optical. One of the two acoustical modes, $\tilde{\omega}_3$, is longitudinal and arises from the quantization of the Q_z component, and the other is a torsional mode, $\tilde{\omega}_2$, and arises from Q_θ; they have velocities near $q = 0$ of $v_3 = 24.3$ km/s and $v_2 = 13.95$ km/s, respectively. Both acoustical modes transform as A_{2u}, and all optical modes as A_{1g}. The higher two optical modes, $\tilde{\omega}_5$ and $\tilde{\omega}_6$, which arise from relative coordinates q_θ and q_z, are 1600 and 1593 cm^{-1}, respectively, and Raman active. These two modes mix each other at about $q = 0.25/c$ and keep their optical characters all along the Brillouin zone. The remaining two optical modes, $\tilde{\omega}_1$ and $\tilde{\omega}_4$, take place at 190 and 865 cm^{-1} at $q = 0$ and arise from the coordinates Q_ρ and q_ρ, respectively. In the present approach, the lower mode $\tilde{\omega}_1$ crosses the two acoustical modes, while the other one $\tilde{\omega}_4$

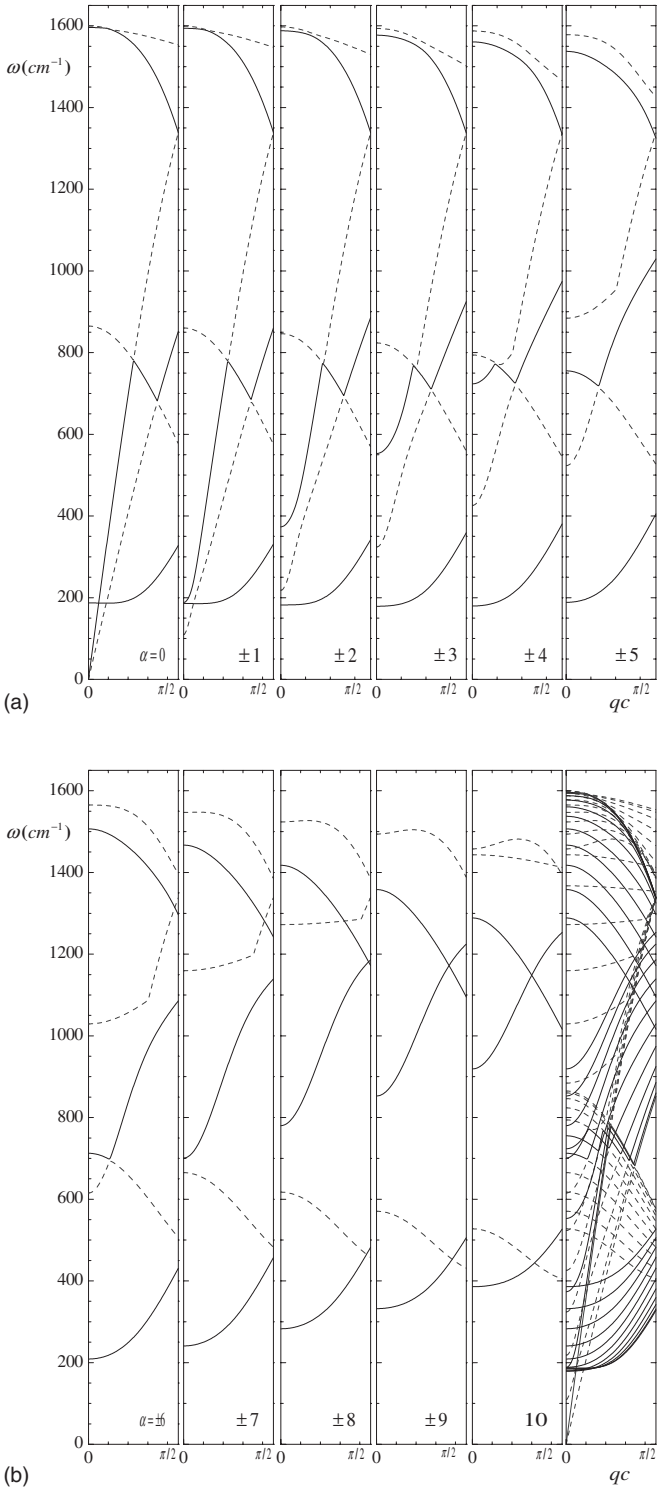

FIG. 4. Plot of $\tilde{\omega}_i(\boldsymbol{q})$ according to Eq. (33) for (a) $\alpha = 0, \pm 1, \pm 2, \pm 3, \pm 4, \pm 5$ and (b) $\alpha = \pm 6, \pm 7, \pm 8, \pm 9, 10$ and their collection into a single panel.

mixes with them. The former case does not agree with the result of Mahan and Jeon, Ref. 16.

For $\alpha=10$, we get the other six nondegenerate modes which are all optical characters, and it appears that we get mode crossings instead of mode mixing, contrary to the results of Mahan and Jeon. If we examine behaviors of $\tilde{\omega}_i$ from $\alpha=1$ to $\alpha=9$, we see that complete mode mixing is present up to $\alpha=7$, and then crossings, two by two, appear. The absence of mode mixing is due to the chosen form of transformations and to omission of certain nonlinear terms.

We should also point out that solutions given by Eq. (33) to cubic equation for each α are strictly divided into two parts; while in one part $\tilde{\omega}_1$, $\tilde{\omega}_5$, and $\tilde{\omega}_6$ modes are involved, the other contains $\tilde{\omega}_2$, $\tilde{\omega}_3$, and $\tilde{\omega}_4$ modes. We see that only the modes in the same part are mixed, but in different parts are crossed.

The modes for $\alpha=1$ are of particular importance, since one of these is doubly degenerate flexure mode, which has an E_{2u} symmetry. This has been observed in many investigations, and its existence is now very well established. In the present work, this mode did not come out as an acoustical branch but it appears to have a finite value at $q=0$, as seen in Fig. 4. Furthermore, as is clearly seen from Figs. 3 and 4(b), respectively, our results, first, do not show up a gradual increase in the highest longitudinal optical (LO) phonon branch when moving away from the Γ point of the Brillouin zone (BZ), and, second, fail to predict the lowest LO phonon mode for $\alpha=\pm 2$ at the Γ point, which is approximately 14 times larger than the 12.6 cm^{-1} found by Jeon and Mahan.[23] In particular, the former, i.e., the highest LO phonon branch itself, is of great importance. When moving away from the Γ point toward the boundary of the BZ, upward curvature of the highest LO phonon dispersion is referred as the overbending feature and is attributed to the origin of the sharp peak in Raman spectrum.[14,15,18,19] As is seen from Fig. 3, while results of Ref. 16 predict a difference between the highest LO phonon frequency and the Γ point one as 104.84 cm^{-1}, our result flattens in the vicinity of the Γ point and then drops without showing a local maximum. However, we think that, as indicated by Maultzsch *et al.*,[18] including the interactions up to fourth order would help reproduce the experimentally observed overbending in the optical phonon modes.

Nevertheless, we think that the ignorance of certain bilinear phonon terms in the proposed diagonalization procedure is the main obstacle in obtaining flexure mode and also showing an anticrossing behavior of the related phonon branches in the low energy region near the Γ point for small values of circumferential quantum number α. We know that Landau's noncrossing theorem does not admit to such a crossing of the levels having the same symmetry, and also it tells us that, if there are two intersecting levels having the same symmetry following an approximate calculation, they will be found to move apart from each other after applying the next approximation[47] (see also Refs. 48 and 49 for recent discussions).

IV. ELECTRON-PHONON INTERACTION

The electron-phonon interaction is obtained from the hopping interaction between carbon atoms: $J_0(\delta\boldsymbol{Q})=J_0+J_1\boldsymbol{\delta}\cdot\delta\boldsymbol{Q}$, where $\delta\boldsymbol{Q}$ is the relative displacements of the neighboring atoms.[30] Contrary to the phonon part, only the first-nearest-neighbor and bond bending interactions are to be considered in the electron-phonon interaction.

A. Nearest-neighbor interactions

Here, as discussed in phonons, if one considers the carbon atom A at the site j, then there are three nearest-neighbor B atoms and the interaction term becomes

$$H^I_{el\text{-}ph}=J_1\sum_{j\delta}[\boldsymbol{\delta}\cdot(\boldsymbol{Q}_{B,j+\delta}-\boldsymbol{Q}_{A,j})](C^\dagger_{A,j}C_{B,j+\delta}+C^\dagger_{B,j+\delta}C_{A,j}), \tag{34}$$

where $C^\dagger$ (C) are the creation (annihilation) operator for electrons. $C^\dagger_{A(B),j}C_{B(A),j}$ terms in Eq. (34) indicate that an electron hops from the carbon atom B (A) to neighboring A (B). Transition from the site representation to a wave vector system is achieved by the transformation

$$C_{B,j+\delta_i}=\frac{1}{\sqrt{nN}}\sum_{\boldsymbol{k}\equiv(k,\gamma)}e^{i(kcl+\gamma\theta_j)}C_{B,\boldsymbol{k}}e^{i\beta^0_i(k,\gamma)}, \tag{35}$$

where N is the number of atoms in a unit cell and $\beta^0_i(k,\gamma)$ are phase factors and given by $\beta^0_1(k,\alpha)=\alpha\theta_1$, $\beta^0_2(k,\alpha)=kc-\alpha\theta_2$, and $\beta^0_3(k,\alpha)=-kc-\alpha\theta_2$, respectively. As k is the wave vector for electrons along the direction of the tube axis, γ is a quantum number of the electrons along the circumference direction of the tube and takes the same values as α. Similarly, if we use Eqs. (5) and (6) for the phonon coordinates, then the interaction term becomes

$$H^I_{el\text{-}ph}=\frac{J_1}{\sqrt{Nn}}\sum_i\sum_{\boldsymbol{q}\equiv(q,\alpha)}\sum_{\boldsymbol{k}\equiv(k,\gamma)}[C^\dagger_{A,k+q,\gamma+\alpha}C_{B,k\gamma}e^{i\beta^0_i(k,\gamma)}+C^\dagger_{B,k+q,\gamma+\alpha}C_{A,k\gamma}e^{-i\beta^0_i(k+q,\gamma+\alpha)}]\tilde{\chi}^{(i)1}_{\boldsymbol{q}}. \tag{36}$$

If the property $\beta^0_i(k+q,\gamma+\alpha)=\beta^0_i(k,\gamma)+\phi^0_i(q,\alpha)$ between phases is used, then Eq. (36) is expressed in a more compact form as follows:

$$H^I_{el\text{-}ph}=\frac{J_1}{\sqrt{Nn}}\sum_{\boldsymbol{q}\equiv(q,\alpha)}\sum_{\boldsymbol{k}\equiv(k,\gamma)}\sum_{l=0}^{1}(C^\dagger_{A,k+q,\gamma+\alpha}C_{B,k\gamma}+(-1)^lC^\dagger_{B,k+q,\gamma+\alpha}C_{A,k\gamma})\mathcal{G}_\ell, \tag{37}$$

where $\mathcal{G}_\ell$ represents the functions $\Sigma\underline{\chi}^{(i)}_{\boldsymbol{q}}\cos\varsigma_i$ and $\Sigma i\underline{\chi}^{(i)}_{\boldsymbol{q}}\sin\varsigma_i$ for $\ell=0$ and 1, respectively. While the former denotes the intraband scattering of an electron from the carbon atom A (B) with wave vector $\boldsymbol{k}\equiv(k,\gamma)$ to the state with wave vector $\boldsymbol{q}+\boldsymbol{k}\equiv(q+k,\alpha+\gamma)$ of the carbon atom A (B), the latter one corresponds to the interband scattering of an electron from the carbon atom A (B) with wave vector $\boldsymbol{k}\equiv(k,\gamma)$ to the state with wave vector $\boldsymbol{q}+\boldsymbol{k}\equiv(q+k,\alpha+\gamma)$ of the carbon atom B (A). $\varsigma_i=\beta^0_i(k,\gamma)+[\phi^0_i(q,\alpha)/2]$, and $i=1,2,3$ refer to Q_ρ, Q_θ, Q_z and $i=4,5,6$ to q_ρ,q_θ,q_z in $\tilde{\chi}^{(i)}_{\boldsymbol{q}}$, respectively, and $\underline{\chi}^{(i)}_{\boldsymbol{q}}$ in Eq. (37) is given by $\underline{\chi}^{(i)}_{\boldsymbol{q}}=\exp[-i\phi^0_i(q,\alpha)/2]\tilde{\chi}^{(i)}_{\boldsymbol{q}}$. If we now use creation and annihilation operators in Q_i coordinates by means of Eq. (14), then the interaction term [Eq. (37)] becomes

$$H_{el\text{-}ph}^{I} = \sum_{\boldsymbol{q}\equiv(q,\alpha)} \sum_{\boldsymbol{k}\equiv(k,\gamma)} \sum_{i=1}^{6} \sum_{l=0}^{1} \mathbb{M}_i^{\mathrm{I}(l)}(\boldsymbol{q},\boldsymbol{k})[C^{\dagger}_{A,k+q,\gamma+\alpha} C_{B,k\gamma} + (-1)^l C^{\dagger}_{B,k+q,\gamma+\alpha} C_{A,k\gamma}](a^{\dagger}_{\boldsymbol{q}i} + a_{\boldsymbol{q}i}), \tag{38}$$

where the electron-phonon interaction strength $\mathbb{M}_i^{\mathrm{I}\pm}(\boldsymbol{q},\boldsymbol{k})$, as $+$ for $l=0$ and $-$ for $l=1$, is defined by

$$\mathbb{M}_i^{\mathrm{I}\pm}(\boldsymbol{q},\boldsymbol{k}) = J_1 \left(\frac{\hbar}{nNM}\right)^{1/2} \frac{\mathbb{A}_i^{\pm}}{2} \frac{1}{\sqrt{\omega_i(\boldsymbol{q})}}, \tag{39}$$

with the coefficients $\mathbb{A}_i^{\pm}$. It can be seen in Appendix B that $\mathbb{A}_i^{\pm}$'s given by Eq. (B1) depend on $\boldsymbol{q},\boldsymbol{k}$ and the structural angles θ_1 and θ_2.

B. Radial bond bending

We adopt a similar procedure to obtain the electron-phonon interaction due to bond bending forces. As in the case of phonon modes, there are two main terms arising from the interactions of an A atom and neighboring three B atoms and a B atom neighboring three A atoms, which are written as follows:

$$H_{el\text{-}ph}^{BB} = J_1 \sum_{j\delta} [\boldsymbol{n}^{\mathrm{I}} \cdot (\boldsymbol{Q}_{Bj+\delta} - \boldsymbol{Q}_{Aj})(C^{\dagger}_{A,j} C_{B,j+\delta} + C^{\dagger}_{B,j+\delta} C_{A,j}) + \boldsymbol{n}^{\mathrm{II}} \cdot (\boldsymbol{Q}_{Aj+\delta} - \boldsymbol{Q}_{Bj})(C^{\dagger}_{B,j} C_{A,j+\delta} + C^{\dagger}_{A,j+\delta} C_{B,j})], \tag{40}$$

with

$$\begin{aligned} &\boldsymbol{n}^{\mathrm{I(II)}} \cdot (\boldsymbol{Q}_{B(A)j+\delta_i} - \boldsymbol{Q}_{A(B)j}) \\ &= \frac{1}{\sqrt{nN}} \sum_{\boldsymbol{q}\equiv(q,\alpha)} \boldsymbol{n}^{\mathrm{I(II)}} \cdot [\boldsymbol{Q}_{B(A)}^{(i)}(\boldsymbol{q}) e^{i\phi_i^0(q,\alpha)} - \boldsymbol{Q}_{A(B)} \\ &\times(\boldsymbol{q})] \exp[i(qc\ell + \alpha\theta_j)] \\ &= \frac{1}{\sqrt{nN}} \sum_{\boldsymbol{q}\equiv(q,\alpha)} \tilde{\chi}_{\mathrm{I(II)}}^{(i)} \exp[i(qc\ell + \alpha\theta_j)]. \end{aligned} \tag{41}$$

By introducing new phases ϵ_i, ϵ_i', and ϵ_i'', which are given by $\epsilon_1(k,\gamma) = \gamma\theta_1$, $\epsilon_2(k,\gamma) = -\gamma\theta_2 + kc$, and $\epsilon_3(k,\gamma) = -\gamma\theta_2 - kc$, $\epsilon_i' = \gamma\theta_1$, and $\epsilon_1'' = \gamma\theta_1$, $\epsilon_2'' = \gamma\tilde{\theta} + kc$, and $\epsilon_3'' = \gamma\tilde{\theta} - kc$, respectively, Eq. (40) can be written as a sum of two terms, $H_{el\text{-}ph}^{BB} = \mathcal{H}_A + \mathcal{H}_B$, where these terms are

$$\mathcal{H}_A = \frac{J_1}{\sqrt{nN}} \sum_i \sum_{\boldsymbol{q}\equiv(q,\alpha)} \sum_{\boldsymbol{k}\equiv(k,\gamma)} \tilde{\chi}_{\mathrm{I}}^{(i)} [C^{\dagger}_{Ak+q,\gamma+\alpha} C_{Bk\gamma} e^{i\epsilon_i(k,\gamma)} + C^{\dagger}_{Bk+q,\gamma+\alpha} C_{Ak\gamma} e^{-i\epsilon_i(k+q,\gamma+\alpha)}], \tag{42}$$

$$\mathcal{H}_B = \frac{J_1}{\sqrt{nN}} \sum_i \sum_{\boldsymbol{q}\equiv(q,\alpha)} \sum_{\boldsymbol{k}\equiv(k,\gamma)} \tilde{\chi}_{\mathrm{II}}^{(i)} \times [C^{\dagger}_{Bk+q,\gamma+\alpha} C_{Ak\gamma} e^{-i\epsilon_i'(k+q,\gamma+\alpha)} e^{i\epsilon_i''(k,\gamma)} + C^{\dagger}_{Ak+q,\gamma+\alpha} C_{Bk\gamma} e^{i\epsilon_i'(k,\gamma)} e^{-i\epsilon_i''(k+q,\gamma+\alpha)}]. \tag{43}$$

It should be noted that these phases satisfy the following relation: $\epsilon_i(k+q,\gamma+\alpha) = \epsilon_i(k,\gamma) + \phi_i^0(q,\alpha)$. Similar to the nearest-neighbor interaction, after calculating $\tilde{\chi}_{\mathrm{I}}^{(i)}$ and $\tilde{\chi}_{\mathrm{II}}^{(i)}$ and then replacing them back into $\mathcal{H}_A$ and $\mathcal{H}_B$ yield the same equation as in the nearest neighbor interaction Hamiltonian, i.e., Eq. (37), provided that $\mathcal{G}_\ell$ now represents the functions $\Sigma'[\underline{\chi}_{\mathrm{I}}^{(i)} \cos(\varsigma_i) + \underline{\chi}_{\mathrm{II}}^{(i)} \cos(\xi_i)]$ and $i\Sigma'[\underline{\chi}_{\mathrm{I}}^{(i)} \sin(\varsigma_i) + \underline{\chi}_{\mathrm{II}}^{(i)} \sin(\xi_i)]$, for $\ell=0$ and 1, respectively, with $\xi_i = \gamma\theta_1 + (\alpha\theta_1/2) - \epsilon_i''(k,\gamma) - [\epsilon_i''(q,\alpha)/2]$. Here, the prime over the sums indicates that $i=3,6$, i.e., the z components of Q and q, respectively, should be excluded from the sums, since, by $i=1,2$, we intend the coordinates Q_ρ, Q_θ and, by $i=4,5$, the coordinates q_ρ, q_θ, respectively. We note that in case of the bond bending interactions, the coefficients containing coordinates satisfy the following simplified relations: $\underline{\chi}_{\mathrm{II}}^{(1)} = -\underline{\chi}_{\mathrm{I}}^{(1)} \times \exp(-\phi_1^0(q,\alpha)/2)$, $\underline{\chi}_{\mathrm{II}}^{(2)} = -\underline{\chi}_{\mathrm{I}}^{(3)}$, and $\underline{\chi}_{\mathrm{II}}^{(3)} = -\underline{\chi}_{\mathrm{I}}^{(2)}$. Finally, after the introduction of creation and annihilation operators, the interaction Hamiltonian becomes

$$H_{el\text{-}ph}^{BB} = \sum_{\boldsymbol{q}\equiv(q,\alpha)} \sum_{\boldsymbol{k}\equiv(k,\gamma)} \sum_i {}' \sum_{l=0}^{1} \mathbb{M}_i^{\mathrm{BB}(\ell)}(\boldsymbol{q},\boldsymbol{k})[C^{\dagger}_{A,k+q,\gamma+\alpha} C_{B,k\gamma} + (-1)^l C^{\dagger}_{B,k+q,\gamma+\alpha} C_{A,k\gamma}](a^{\dagger}_{\boldsymbol{q}i} + a_{\boldsymbol{q}i}), \tag{44}$$

where the interaction strength $\mathbb{M}_i^{\mathrm{BB}(\ell)}(\boldsymbol{q},\boldsymbol{k})$ is defined, in the same way as the nearest neighbor interaction, by the relation

$$\mathbb{M}_i^{\mathrm{BB}(\ell)}(\boldsymbol{q},\boldsymbol{k}) = J_1 \left(\frac{\hbar}{nNM}\right)^{1/2} \frac{\mathbb{D}_i^{\pm}}{2} \frac{1}{\sqrt{\omega_i(\boldsymbol{q})}}, \tag{45}$$

with the $\mathbb{D}_i^{\pm}$ elements given in Appendix B. Here, contrary to the nearest neighbor interaction, $\mathbb{D}_i^{\pm}$ given by Eq. (B2) depend only on the structural angles, and not on the q and k wave vectors. The dependence on $\boldsymbol{q}$ and $\boldsymbol{k}$ of $\mathbb{M}_i^{\mathrm{BB}(\ell)}(\boldsymbol{q},\boldsymbol{k})$ enters through the $\omega_i(\boldsymbol{q})$ frequency.

C. Results

Although we have obtained the electron-phonon interactions in analytical form, it is not still complete to use in any application since the phonon part of the general Hamiltonian underwent two successive unitary transformations for diagonalization procedure. Therefore, it is necessary to exploit the same unitary transformations for the interaction parts as well, so that we can, first, get rid of the dummy frequency $\omega_i(\boldsymbol{q})$ and then obtain a renormalized frequency in accordance with the phonon dispersion.

After the first transformation U_1, the phonon operator part of the interaction terms comprises a factor $(\cosh 2\lambda_i - \sinh 2\lambda_i)^{1/2} = [\omega_i(\boldsymbol{q})/\omega_i^{(0)}(\boldsymbol{q})]^{1/2}$ and transforms as $a^{\dagger}_{\boldsymbol{q}i} + a_{\boldsymbol{q}i} \rightarrow \tilde{a}^{\dagger}_{\boldsymbol{q}i} + \tilde{a}_{\boldsymbol{q}i} = (\cosh 2\lambda_i - \sinh 2\lambda_i)^{1/2}(a^{\dagger}_{\boldsymbol{q}i} + a_{\boldsymbol{q}i})$. This eliminates the dummy frequency $\omega_i(\boldsymbol{q})$ and renormalizes the interaction strength as $\tilde{\mathbb{M}}_i^{\mathrm{I}\pm}(\boldsymbol{q},\boldsymbol{k}) = [\omega_i(\boldsymbol{q})/\omega_i^{(0)}(\boldsymbol{q})]^{1/2} \mathbb{M}_i^{\mathrm{I}\pm}(\boldsymbol{q},\mathbf{k})$, and furthermore we divide this result by the Raman frequency $\hbar\omega_0$ to make it dimensionless. We follow the same procedure what we have done in the phonon part, i.e., we distinguish the ith component from the other five distinct ones. Therefore, we write $H_{el\text{-}ph,i}^{tot} = H_{el\text{-}ph,i} + \Sigma_{j(\neq i)} H_{el\text{-}ph,j}$ wherein

$$H_{el\text{-}ph,i} = \sum_{\boldsymbol{q}\equiv(q,\alpha)} \sum_{\boldsymbol{k}\equiv(k,\gamma)} \sum_{l=0}^{1} \bar{\mathbb{M}}_i^{\mathrm{T}(\ell)}(\boldsymbol{q},\boldsymbol{k})[C^\dagger_{A,k+q,\gamma+\alpha} C_{B,k\gamma} + (-1)^l C^\dagger_{B,k+q,\gamma+\alpha} C_{A,k\gamma}](a^\dagger_{\boldsymbol{q}i} + a_{\boldsymbol{q}i}), \tag{46}$$

where

$$\bar{\mathbb{M}}_n^{\mathrm{T}(\ell)}(\boldsymbol{q},\boldsymbol{k}) = \frac{J_1}{\hbar\omega_0}\left(\frac{\hbar}{nNM}\right)^{1/2}\frac{1}{2}(\mathbb{A}_n^{\pm} + \mathbb{D}_n^{\pm})\frac{1}{\sqrt{\omega_n(\boldsymbol{q})}}, \tag{47}$$

in which the second term in parentheses takes nonzero values for $i \neq 3,6$ otherwise it should be treated as zero. Since the second transformation changes $a^\dagger_{\boldsymbol{q}i} + a_{\boldsymbol{q}i}$ and $a^\dagger_{\boldsymbol{q}j} + a_{\boldsymbol{q}j}$, according to Eqs. (22) and Eq. (23), the interaction with the mode i can then be written as

$$\mathcal{M}_i^{\mathrm{T}(\ell)}(\boldsymbol{q},\boldsymbol{k}) = \cos\Lambda \bar{\mathbb{M}}_i^{\mathrm{T}(\ell)}(\boldsymbol{q},\boldsymbol{k}) + \sum_{j(\neq i)} \bar{\lambda}_j \sin\Lambda \bar{\mathbb{M}}_j^{\mathrm{T}(\ell)} \tag{48}$$

$$\mathcal{M}_j^{\mathrm{T}(\ell)}(\boldsymbol{q},\boldsymbol{k}) = \bar{\mathbb{M}}_j^{\mathrm{T}(\ell)}(\boldsymbol{q},\boldsymbol{k}) - \bar{\lambda}_j \sin\Lambda \bar{\mathbb{M}}_i^{\mathrm{T}(\ell)}(\boldsymbol{q},\boldsymbol{k}) - \sum_{k(\neq i,j)} \bar{\lambda}_j\bar{\lambda}_k(1-\cos\Lambda)\bar{\mathbb{M}}_k^{\mathrm{T}(\ell)}. \tag{49}$$

Here, $\cos\Lambda$ and $\sin\Lambda$ are known from the phonon parts, and they can easily be found as $\sin\Lambda = \pm\sqrt{F/(1+F)}$ and $\cos\Lambda = \pm 1/\sqrt{(1+F)}$, where F is defined to be

$$F = \sum_{j\neq i}^{6} \frac{1}{[\tilde{\omega}_i(\boldsymbol{q}) - \bar{\omega}_j^{(0)}(\boldsymbol{q})]^2}\left[\frac{\tilde{\omega}_{ij}^{(0)}(\boldsymbol{q})}{2}\right]^2.$$

Furthermore, $\bar{\lambda}_j \sin\Lambda$ in Eqs. (48) and (49) is given by

$$\bar{\lambda}_j \sin\Lambda = \frac{1}{\tilde{\omega}_i(\boldsymbol{q}) - \bar{\omega}_j^{(0)}(\boldsymbol{q})}\left[\frac{\tilde{\omega}_{ij}^{(0)}(\boldsymbol{q})}{2}\cos\Lambda + \Delta_j \sin\Lambda\right]. \tag{50}$$

Thus, we have obtained a Fröhlich-type Hamiltonian that has the phonon part arising from nearest-neighbor, next-nearest-neighbor, and bond bending interactions and the electron-phonon interaction part, which is comprised of nearest-neighbor and bond bending interactions:

$$H = J_0 \sum_{j\equiv(m\ell)} \sum_{\delta_i} [C^\dagger_{B,j+\delta_i} C_{A,j} + C^\dagger_{A,j} C_{B,j+\delta_i}] + \sum_i H_i,$$

with

$$H_i = \sum_{\boldsymbol{q}\equiv(q,\alpha)} \hbar\tilde{\omega}_i(\boldsymbol{q})\left(a^\dagger_{\boldsymbol{q}i}a_{\boldsymbol{q}i} + \frac{1}{2}\right) + \tilde{H}_{el\text{-}ph,i} + \sum_{j(\neq i)} \tilde{H}_{el\text{-}ph,j},$$

$$\tilde{H}_{el\text{-}ph,i} = \sum_{\boldsymbol{q}\equiv(q,\alpha)} \sum_{\boldsymbol{k}\equiv(k,\gamma)} \sum_{l=0}^{1} \mathcal{M}_i^{\mathrm{T}(\ell)}(\boldsymbol{q},\boldsymbol{k})[C^\dagger_{A,k+q,\gamma+\alpha} C_{B,k\gamma} + (-1)^l C^\dagger_{B,k+q,\gamma+\alpha} C_{A,k\gamma}](a^\dagger_{\boldsymbol{q}i} + a_{\boldsymbol{q}i}),$$

where one can drop the third term in H_i since it represents a further nondiagonality. As a final remaining task, we shall now briefly discuss the effect of the diagonalization of H_{el} onto the electron-phonon interaction part found above. To achieve this, we will propose a third unitary transformation acting on fermion operators. However, before doing this, we should apply the routine procedure for the well-known tight-binding Hamiltonian given in the Sec. I, i.e., by performing the sum over the nearest neighbors, then tight-binding Hamiltonian takes the following form:

$$H_{el} = J_0 \sum_{\boldsymbol{k}\equiv(k,\gamma)} [C^\dagger_{A,k,\gamma} C_{B,k,\gamma}\Theta(\boldsymbol{k}) + \Theta^*(\boldsymbol{k}) C^\dagger_{B,k,\gamma} C_{A,k,\gamma}], \tag{51}$$

with $\Theta(\boldsymbol{k}) = \Sigma_{i=1}^{3} \exp[i\beta_i(\boldsymbol{k})] = |\Theta(\boldsymbol{k})|\exp(i\xi)$. Now, H_{el} can be diagonalized by introducing a third unitary transformation as $U_3 = \exp[S_3(\boldsymbol{k})]$, with $S_3(\boldsymbol{k}) = \lambda C^\dagger_{A,\boldsymbol{k}} C_{B,\boldsymbol{k}} - \lambda^* C^\dagger_{B,\boldsymbol{k}} C_{A,\boldsymbol{k}}$, under which the fermion operators $C_{A,\boldsymbol{k}}$ and $C_{B,\boldsymbol{k}}$ transform as[39] $\tilde{C}_{A(B),\boldsymbol{k}} = C_{A(B),\boldsymbol{k}}\cos|\lambda| \mp C_{B(A),\boldsymbol{k}}\exp(\mp i\zeta)\sin|\lambda|$, where $\lambda = |\lambda|\exp(+i\zeta)$ is used. Here, the upper sign belongs to those given in subscript parentheses. Therefore, the resulting Hamiltonian $\tilde{H}_{el} = U_3^{-1} H_{el} U_3$ can be diagonalized by choosing $|\lambda| = \pi/4$ and $\zeta = \xi$, yielding energies $E^{(\pm)} = \pm J_0|\Theta(\boldsymbol{k})|$. In fact, this choice of parameters corresponds to the well-known Bogoliubov transformation, used in Ref. 30, as well. It should also be pointed out that the variation of the expectation value of $\tilde{H}_{el}$ by the fermionic ground state, i.e., $\langle\tilde{H}_{el}\rangle_0$, with respect to both $|\lambda|$ and ζ, respectively, gives the same condition for diagonalization. Hence, Eq. (51) becomes

$$H_{el} = \sum_{\boldsymbol{k}\equiv(k,\gamma)} [E^{(-)} C^\dagger_{A,k,\gamma} C_{A,k,\gamma} + E^{(+)} C^\dagger_{B,k,\gamma} C_{B,k,\gamma}],$$

which is the well-known tight-binding result, i.e., $E^{(\pm)} = \pm J_0|\Theta(\boldsymbol{k})| = \pm J_0\sqrt{1 + 4\cos^2(kc) + 2\cos(kc)2\cos(\gamma\tilde{\theta})}$. If one transforms the electron-phonon interaction Hamiltonian given by $H^{tot}_{el\text{-}ph,i}$ in the same way and performs the sum over ℓ, then the result turns out to be

$$H^{tot}_{el\text{-}ph,i} = \sum_{\boldsymbol{q}} \sum_{\boldsymbol{k}} \left[\mathcal{D}_i(\boldsymbol{k},\boldsymbol{q})(a^\dagger_{\boldsymbol{q}i} + a_{\boldsymbol{q}i}) + \sum_{j(\neq i)} \mathcal{D}_j(\boldsymbol{k},\boldsymbol{q})(a^\dagger_{\boldsymbol{q}j} + a_{\boldsymbol{q}j})\right], \tag{52}$$

where we have defined the operator

$$\mathcal{D}_\ell(\boldsymbol{k},\boldsymbol{q}) = [\mathcal{L}_\ell^{(-)} C^\dagger_{B,\boldsymbol{k}+\boldsymbol{q}} C_{B,\boldsymbol{k}} - \mathcal{L}_\ell^{(+)} C^\dagger_{A,\boldsymbol{k}+\boldsymbol{q}} C_{A,\boldsymbol{k}}] + \exp(+i\xi) \times [\mathcal{L}_\ell^{(+)} C^\dagger_{A,\boldsymbol{k}+\boldsymbol{q}} C_{B,\boldsymbol{k}} + \exp(-i\xi)\mathcal{L}_\ell^{(-)} C^\dagger_{B,\boldsymbol{k}+\boldsymbol{q}} C_{A,\boldsymbol{k}}],$$

with $\Psi_\pm = \{\exp[-i\xi(\boldsymbol{k})] \pm \exp[+i\xi(\boldsymbol{k}+\boldsymbol{q})]\}/2$ and $\mathcal{L}_i^{(\pm)} = \mathcal{M}_i^{\mathrm{T}(+)}\Psi_+^* \pm \mathcal{M}_i^{\mathrm{T}(-)}\Psi_-^*$. To gain a further insight into Eq. (52), one considers the case $\gamma = 0$ for the electron states. Since it corresponds to taking $\exp[i\xi(\boldsymbol{k})] = 1$, hence $\Psi_- = 0$ and $\Psi_+ = 1$, and finally the total Hamiltonian becomes

$$H = \sum_k [E^{(+)} C^\dagger_{A,k} C_{A,k} + E^{(-)} C^\dagger_{B,k} C_{B,k}] + \sum_i \sum_{\boldsymbol{q}} \left\{ \hbar \tilde{\omega}_i(\boldsymbol{q}) \left(a^\dagger_{\boldsymbol{q}i} a_{\boldsymbol{q}i} + \frac{1}{2} \right) + \sum_k \left[\mathcal{D}_i(k,\boldsymbol{q})(a^\dagger_{\boldsymbol{q}i} + a_{\boldsymbol{q}i}) + \sum_{j(\neq i)} \mathcal{D}_j(k,q)(a^\dagger_{\boldsymbol{q}j} + a_{\boldsymbol{q}j}) \right] \right\}, \tag{53}$$

with

$$\mathcal{D}_\ell(k,q) = \mathcal{M}^{\mathrm{T}(+)}_\ell (C^\dagger_{B,\boldsymbol{k}+\boldsymbol{q}} C_{B,\boldsymbol{k}} - C^\dagger_{A,\boldsymbol{k}+\boldsymbol{q}} C_{A,\boldsymbol{k}}) + \mathcal{M}^{\mathrm{T}(-)}_\ell \times (C^\dagger_{A,\boldsymbol{k}+\boldsymbol{q}} C_{B,\boldsymbol{k}} - C^\dagger_{B,\boldsymbol{k}+\boldsymbol{q}} C_{A,\boldsymbol{k}}),$$

while the first term in the electron-phonon interaction part represents the intraband transitions and the other one corresponds to interband transitions. It should be noted that sum over k in Eq. (53) refers to the case with $\gamma=0$.

V. SUMMARY AND CONCLUSION

In conclusion, we presented a detailed investigation for phonon dispersion relations and electron-phonon interactions in armchair SWCTs, in which we found analytical expressions for phonon modes and a Fröhlich-type Hamiltonian. Our approach was based on mass and spring model, originally developed in Refs. 16 and 30 with incorporation of bond bending potentials, but we furthered classical lattice vibrations to obtain fully quantized phonon modes. After quantization, the phonon Hamiltonian contained phonon creation and annihilation operators in quadratic forms, which were diagonalized by consecutive canonical transformations to obtain phonon frequencies. We have also used the resolvent formalism to get phonon frequencies in analytical forms, where correct roots of phonon modes have been chosen by procedure of the Fano problem. During this procedure, we fixed the Raman line 1600 cm^{-1} and used the same values of spring constants as in Refs. 16 and 30 to obtain other modes of the full spectrum.

We also obtained electron-phonon interaction terms from the hopping interaction between carbon atoms, where we considered only nearest-neighbor and bond bending interactions. Here, we employed the same canonical transformations as the phonon part so that they comprised the correct frequencies of phonon modes. This gave us the coupling strength in terms of the frequencies $\tilde{\omega}_i$, the wave vector q, the quantum numbers α, the angles θ_1 and θ_2, the chiral numbers (n,n), and the hopping parameters J_0 and J_1. It should be noted that the contribution coming from the bond bending did not have q dependence.

The comparison of our analytical results with the existing literature is reasonably good but not perfect, especially in that they fail to predict flexure mode and the lowest LO phonon branch correctly and, for small values of circumferential quantum number α, yield a crossing behavior of phonon modes in the low energy region. We trace the inadequacy in this region back to the choice of canonical transformations and omission of certain quadratic terms in the diagonalization procedure. Perhaps, implementation of a more sophisticated additional unitary transformation may be needed at this stage so as to improve this unsatisfactory point.

We conclude by pointing out various implications for the framework developed in the present paper. Here, we have been solely concerned with one type of SWCNTs, namely, armchair. Extensions to zigzag and chiral SWCNTs, as well, can be achieved by just taking their special geometries of these nanostructures into account. Further, our consideration can also be extended to graphene.

APPENDIX A

The nonzero coefficients of the matrix $\mathbb{A}^{(1)}$ for the nearest-neighbor interactions required to calculate the relevant lattice potential given by Eqs. (12) are given in this appendix. They are calculated with the aid of explicit expressions $\tilde{\chi}^{(i)}$ factors given in Eq. (9) as

$$\mathbb{A}^{(1)}_{11} = \mathbb{A}^{(1)}_{44} = (s^0_1)^2 + [(s^0_2)^2/2],$$

$$\mathbb{A}^{(1)}_{22} = \mathbb{A}^{(1)}_{55} = (c^0_1)^2 + [(c^0_2)^2/2],$$

$$\mathbb{A}^{(1)}_{33} = \mathbb{A}^{(1)}_{66} = 3/2, \tag{A1}$$

for diagonal ones, and

$$\mathbb{A}^{(1)}_{12} = \mathbb{A}^{(1)}_{45} = -s^0_1 c^0_1 + [s^0_2 c^0_2/2],$$

$$\mathbb{A}^{(1)}_{14} = (s^0_1)^2 \exp(i\alpha\theta_1) + [(s^0_2)^2 \exp(-i\alpha\theta_2) c^0_q/2],$$

$$\mathbb{A}^{(1)}_{15} = -\mathbb{A}^{(1)}_{24} = c^0_1 s^0_1 \exp(i\alpha\theta_1) - [c^0_2 s^0_2 \exp(-i\alpha\theta_2) c^0_q/2],$$

$$\mathbb{A}^{(1)}_{25} = -(c^0_1)^2 \exp(i\alpha\theta_1) - [(c^0_2)^2 \exp(-i\alpha\theta_2) c^0_q/2],$$

$$\mathbb{A}^{(1)}_{16} = i\sqrt{3} s^0_2 \exp(-i\alpha\theta_2) s^0_q/2,$$

$$\mathbb{A}^{(1)}_{26} = \mathbb{A}^{(1)}_{35} = i\sqrt{3} c^0_2 \exp(-i\alpha\theta_2) s^0_q/2,$$

$$\mathbb{A}^{(1)}_{34} = -i\sqrt{3} s^0_2 \exp(-i\alpha\theta_2) s^0_q/2,$$

$$\mathbb{A}^{(1)}_{36} = -3 \exp(-i\alpha\theta_2) c^0_q/2, \tag{A2}$$

for the nondiagonal ones. With the same procedure, we find the nonzero coefficients of the matrix $\mathbb{A}^{(2)}$ for the next-nearest-neighbor interactions to be

$$\mathbb{A}^{(2)}_{11} = \mathbb{A}^{(2)}_{44} = 6(\tilde{s}^0)^2 (1 + c^0_q \tilde{c}^0_\alpha),$$

$$\mathbb{A}^{(2)}_{22} = \mathbb{A}^{(2)}_{55} = 6(\tilde{c}^0)^2 (1 - c^0_q \tilde{c}^0_\alpha),$$

$$\mathbb{A}^{(2)}_{33} = \mathbb{A}^{(2)}_{66} = 2[1 - c^0_q \tilde{c}^0_\alpha + 4(s^0_q)^2],$$

$$\mathbb{A}^{(2)}_{12} = \mathbb{A}^{(2)}_{45} = 6i\tilde{s}^0 \tilde{c}^0 \tilde{s}^0_\alpha c^0_q,$$

$$\mathbb{A}^{(2)}_{13} = \mathbb{A}^{(2)}_{46} = 2i\sqrt{3} \tilde{s}^0 s^0_q \tilde{c}^0_\alpha,$$

$$\mathbb{A}_{23}^{(2)} = \mathbb{A}_{56}^{(2)} = 2\sqrt{3}\tilde{c}^0 s_q^0 s_\alpha^0. \tag{A3}$$

Next we perform the same steps for the coefficients related to bond bending interactions,

$$\mathbb{A}_{11}^{(3)} = \mathbb{A}_{44}^{(3)} = |D_1|^2 + |D_3|^2 = 2(c_1^0)^2 + 4(c_2^0)^2[1 + (c_q^0)^2] + 4c_1^0 c_2^0(1 + \tilde{c}_\alpha^0 c_q^0),$$

$$\mathbb{A}_{22}^{(3)} = \mathbb{A}_{55}^{(3)} = |D_2|^2 = (s_1^0)^2[1 - 2\tilde{c}_\alpha^0 c_q^0 + (c_q^0)^2],$$

$$\mathbb{A}_{14}^{(3)} = -D_1^*(D_3 + D_3^*)e^{i\alpha\theta_1} = -2(c_1^0 + 2c_2^0)(c_1^0 e^{i\alpha\theta_1} + 2c_2^0 c_q^0 e^{-i\alpha\theta_2}),$$

$$\mathbb{A}_{15}^{(3)} = -\mathbb{A}_{24}^{(3)} = D_2^* D_3^* e^{i\alpha\theta_1} = s_1^0(c_1^0 + 2c_2^0)(e^{i\alpha\theta_1} - c_q^0 e^{-i\alpha\theta_2}),$$

$$\mathbb{A}_{12}^{(3)} = -\mathbb{A}_{45}^{(3)*} = D_1^* D_2 = s_1^0[c_1^0(1 - \tilde{c}_\alpha^0 c_q^0) - ic_q^0 \tilde{s}_\alpha^0(c_1^0 + 2c_2^0) - 2c_2^0(c_q^0)^2 + 2c_2^0 c_q^0 \tilde{c}_\alpha^0], \tag{A4}$$

with $D_1 = c_1^0 + 2c_2^0 c_q^0 \exp(i\alpha\tilde{\theta})$, $D_2 = s_2^0[1 - c_q^0 \exp(i\alpha\tilde{\theta})]$, and $D_3 = c_1^0 + 2c_2^0$. Note that the coefficients $\mathbb{A}_{ij}^{(k)}$ form a square matrix $\mathbb{A}$ of order 6×6. In this appendix, we will also give the diagonal $\tilde{\mathbb{A}}_{ii}$'s together with the nonzero Re $\tilde{\mathbb{A}}_{ij}$ coefficients, given in Eq. (20):

$$\tilde{\mathbb{A}}_{11} = r_1[2(s_1^0)^2(1 + \tilde{c}_{1\alpha}^0) + (s_2^0)^2(1 + \tilde{c}_{2\alpha}^0 c_q^0)] + 12r_2(\tilde{s}_\alpha^0)^2(1 + \tilde{c}_\alpha^0 c_q^0) + 2r_3[2(c_1^0)^2(1 - \tilde{c}_{1\alpha}^0) + 4(c_2^0)^2(1 + (c_q^0)^2 - 2\tilde{c}_{2\alpha}^0 c_q^0) + 4c_1^0 c_2^0(1 + \tilde{c}_\alpha^0 c_q^0 - \tilde{c}_{2\alpha}^0 c_q^0 - \tilde{c}_{1\alpha}^0)],$$

$$\tilde{\mathbb{A}}_{22} = r_1[2(c_1^0)^2(1 - \tilde{c}_{1\alpha}^0) + (c_2^0)^2(1 - \tilde{c}_{2\alpha}^0 c_q^0)] + 12r_2(\tilde{c}_\alpha^0)^2(1 - \tilde{c}_\alpha^0 c_q^0) + 2r_3(s_1^0)^2[1 + (c_q^0)^2 - 2\tilde{c}_\alpha^0 c_q^0],$$

$$\tilde{\mathbb{A}}_{33} = 3r_1(1 - \tilde{c}_{2\alpha}^0 c_q^0) + 4r_2[1 + 4(s_q^0)^2 - \tilde{c}_\alpha^0 c_q^0],$$

$$\tilde{\mathbb{A}}_{44} = r_1[2(s_1^0)^2(1 - \tilde{c}_{1\alpha}^0) + (s_2^0)^2(1 - \tilde{c}_{2\alpha}^0 c_q^0)] + 12r_2(\tilde{s}_\alpha^0)^2(1 + \tilde{c}_\alpha^0 c_q^0) + 2r_3[2(c_1^0)^2(1 + \tilde{c}_{1\alpha}^0) + 4(c_2^0)^2(1 + (c_q^0)^2 + 2\tilde{c}_{2\alpha}^0 c_q^0) + 4c_1^0 c_2^0(1 + \tilde{c}_\alpha^0 c_q^0 + \tilde{c}_{2\alpha}^0 c_q^0 + \tilde{c}_{1\alpha}^0)],$$

$$\tilde{\mathbb{A}}_{55} = r_1[2(c_1^0)^2(1 + \tilde{c}_{1\alpha}^0) + (c_2^0)^2(1 + \tilde{c}_{2\alpha}^0 c_q^0)] + 12r_2(\tilde{c}_\alpha^0)^2(1 - \tilde{c}_\alpha^0 c_q^0) + 2r_3(s_1^0)^2[1 + (c_q^0)^2 - 2\tilde{c}_\alpha^0 c_q^0],$$

$$\tilde{\mathbb{A}}_{66} = 3r_1(1 + \tilde{c}_{2\alpha}^0 c_q^0) + 4r_2[1 + 4(s_q^0)^2 - \tilde{c}_\alpha^0 c_q^0], \tag{A5}$$

and

$$\left.\begin{matrix}\text{Re } \tilde{\mathbb{A}}_{15} \\ \text{Re } \tilde{\mathbb{A}}_{24}\end{matrix}\right\} = r_1[-2s_1^0 c_1^0(1 + \tilde{c}_{1\alpha}^0) + s_2^0 c_2^0(1 \pm \tilde{c}_{2\alpha}^0 c_q^0)] + 2r_3 s_1^0[c_1^0(1 - \tilde{c}_\alpha^0 c_q^0) - 2c_2^0(c_q^0)^2 \mp (c_1^0 + 2c_2^0) \times (\tilde{c}_{1\alpha}^0 - \tilde{c}_{2\alpha}^0 c_q^0) + 2c_2^0 c_q^0 \tilde{c}_\alpha^0],$$

$$\left.\begin{matrix}\text{Re } \tilde{\mathbb{A}}_{16} \\ \text{Re } \tilde{\mathbb{A}}_{34}\end{matrix}\right\} = \mp \sqrt{3} r_1 s_2^0 s_q^0 \tilde{s}_{2\alpha}^0,$$

$$\left.\begin{matrix}\text{Re } \tilde{\mathbb{A}}_{23} \\ \text{Re } \tilde{\mathbb{A}}_{56}\end{matrix}\right\} = \pm \sqrt{3} r_1 c_2^0 s_1^0 \tilde{s}_{2\alpha}^0 + 4\sqrt{3} r_2 \tilde{c}^0 \tilde{s}_\alpha^0 s_q^0. \tag{A6}$$

APPENDIX B

The coefficients required in calculating the electron-phonon interaction amplitudes for armchair CNTs are given in this appendix. For the electron-phonon interactions, we can represent the relevant equations by the matrix

$$\begin{pmatrix}\mathbb{A}_{1(4)}^{+(-)} \\ \mathbb{A}_{5(2)}^{+(-)}\end{pmatrix} = C_1^{+(-)}\begin{pmatrix}+s_1^0 \\ -c_1^0\end{pmatrix} + C_2^{+(-)}\begin{pmatrix}s_2^0 \\ c_2^0\end{pmatrix},$$

$$\begin{pmatrix}\mathbb{A}_{1(4)}^{-(+)} \\ \mathbb{A}_{5(2)}^{-(+)}\end{pmatrix} = iS_1^{+(-)}\begin{pmatrix}+s_1^0 \\ -c_1^0\end{pmatrix} - iS_2^{+(-)}\begin{pmatrix}s_2^0 \\ c_2^0\end{pmatrix},$$

$$\begin{pmatrix}-i\mathbb{A}_{6(3)}^{-(+)} \\ +\mathbb{A}_{6(3)}^{+(-)}\end{pmatrix} = -\sqrt{3}s_k^0\begin{pmatrix}\tilde{c}_{2\gamma}^0 \\ \tilde{s}_{2\gamma}^0\end{pmatrix} \pm s_{kq}^0\begin{pmatrix}\tilde{c}_{2\alpha\gamma}^0 \\ \tilde{s}_{2\alpha\gamma}^0\end{pmatrix}, \tag{B1}$$

with

$$C_1^\pm = \tilde{c}_{1\gamma}^0 \pm \tilde{c}_{1\alpha\gamma}^0, \quad C_2^\pm = c_k^0 \tilde{c}_{2\gamma}^0 \pm c_{kq}^0 \tilde{c}_{2\alpha\gamma}^0,$$

$$S_1^\pm = \tilde{s}_{1\gamma}^0 \pm \tilde{s}_{1\alpha\gamma}^0, \quad S_2^\pm = c_k^0 \tilde{s}_{2\gamma}^0 \pm c_{kq}^0 \tilde{s}_{2\alpha\gamma}^0.$$

for the nearest neighbor, and

$$\mathbb{D}_1^+/c_1^0 = \mathbb{D}_5^+/s_1^0 = i(-\tilde{s}_{1\alpha}^0 - \tilde{s}_{1\gamma}^0 + \tilde{s}_{1\alpha\gamma}^0) - (1 - \tilde{c}_{1\alpha}^0),$$

$$\mathbb{D}_2^+/s_1^0 = \mathbb{D}_4^+/c_1^0 = -i\tilde{s}_{1\alpha}^0 + (1 + \tilde{c}_{1\alpha}^0 - \tilde{c}_{1\gamma}^0 - \tilde{c}_{1\alpha\gamma}^0),$$

$$\mathbb{D}_1^-/c_1^0 = \mathbb{D}_5^-/s_1^0 = -(\tilde{c}_{1\gamma}^0 - \tilde{c}_{1\alpha\gamma}^0),$$

$$\mathbb{D}_2^-/s_1^0 = \mathbb{D}_4^-/c_1^0 = -i(\tilde{s}_{1\gamma}^0 + \tilde{s}_{1\alpha\gamma}^0), \tag{B2}$$

for bond bending interactions, where we have also defined the following abbreviations: $\tilde{c}_{i\alpha(\gamma)}^0 = \cos(\alpha(\gamma)\theta_i)$, $\tilde{s}_{i\alpha(\gamma)}^0 = \sin(\alpha(\gamma)\theta_i)$, $\tilde{c}_{i\alpha\gamma}^0 = \cos((\alpha+\gamma)\theta_i)$, and $\tilde{s}_{i\alpha\gamma}^0 = \sin((\alpha+\gamma)\theta_i)$, for $i = 1$ and 2, respectively.

[1] S. Iijima, Nature (London) **354**, 56 (1991).
[2] S. Iijima and T. Ichihashi, Nature (London) **363**, 603 (1993).
[3] D. S. Bethune, C. H. Klang, M. S. de Vries, G. Gorman, R. Savoy, J. Vazquez, and R. Beyers, Nature (London) **363**, 605 (1993).
[4] R. Saito, G. Dresselhauss, and M. S. Dresselhaus, *Physical Properties of Carbon Nanotubes* (Imperial College Press, London, 1998).
[5] Z. K. Tang, L. Zhang, N. Wang, X. X. Zhang, G. H. Wen, G. D. Li, J. N. Wang, C. T. Chan, and Ping Sheng, Science **292**, 2462 (2001).
[6] M. Kociak, A. Yu. Kasumov, S. Guéron, B. Reulet, I. I. Khodos, Yu. B. Gorbatov, V. T. Volkov, L. Vaccarini, and H. Bouchiat, Phys. Rev. Lett. **86**, 2416 (2001).
[7] K. Iyakutti, A. Bodapati, X. Peng, P. Keblinsi, and S. K. Nayak, Phys. Rev. B **73**, 035413 (2006).
[8] R. A. Jishi, L. Venkataraman, M. S. Dresselhaus, and G. Dresselhaus, Chem. Phys. Lett. **209**, 77 (1993).
[9] M. S. Dresselhaus and P. C. Eklund, Adv. Phys. **49**, 705 (2000).
[10] G. D. Mahan, Phys. Rev. B **65**, 235402 (2002).
[11] V. N. Popov, V. E. Van Doren, and M. Balkanski, Phys. Rev. B **61**, 3078 (2000).
[12] H. Suzuura and T. Ando, Phys. Rev. B **65**, 235412 (2002).
[13] J. X. Cao, X. H. Yan, Y. Xiao, Y. Tang, and J. W. Ding, Phys. Rev. B **67**, 045413 (2003).
[14] Lin-Hui Ye, Bang-Gui Liu, Ding-Sheng Wang, and Rushan Han, Phys. Rev. B **69**, 235409 (2004).
[15] Daniel Sánchez-Portal, Emilio Artacho, José M. Soler, Angel Rubio, and Pablo Ordejón, Phys. Rev. B **59**, 12678 (1999).
[16] G. D. Mahan and Gun Sang Jeon, Phys. Rev. B **70**, 075405 (2004).
[17] M. Damnjanović, I. Milošević, T. Vuković, and R. Sredanović, Phys. Rev. B **60**, 2728 (1999).
[18] J. Maultzsch, S. Reich, C. Thomsen, E. Dobardžić, I. Milošević, and M. Damnjanović, Solid State Commun. **121**, 471 (2002).
[19] E. Dobardžić, I. Milošević, B. Nikolić, T. Vuković, and M. Damnjanović, Phys. Rev. B **68**, 045408 (2003).
[20] Ivanka Milošević, Edib Dobardžić, and Milan Damnjanović, Phys. Rev. B **72**, 085426 (2005).
[21] Jin-Wu Jiang, Hui Tang, Bing-Shen Wang, and Zhao-Bin Su, Phys. Rev. B **73**, 235434 (2006).
[22] M. S. Dresselhaus, G. Dresselhaus, R. Saito, and A. Jorio, Phys. Rep. **409**, 47 (2005).
[23] Gun Sang Jeon and G. D. Mahan, Phys. Rev. B **72**, 155415 (2005).
[24] U. J. Kim, X. M. Liu, C. A. Furtado, G. Chen, R. Saito, J. Jiang, M. S. Dresselhaus, and P. C. Eklund, Phys. Rev. Lett. **95**, 157402 (2005).
[25] O. E. Alon, Phys. Rev. B **63**, 201403(R) (2001).
[26] M. Machón, S. Reich, H. Telg, J. Maultzsch, P. Ordejón, and C. Thomsen, Phys. Rev. B **71**, 035416 (2005).
[27] R. A. Jishi, M. S. Dresselhaus, and G. Dresselhaus, Phys. Rev. B **48**, 11385 (1993).
[28] L. M. Woods and G. D. Mahan, Phys. Rev. B **61**, 10651 (2000).
[29] Michele Lazzeri, S. Piscanec, Francesco Mauri, A. C. Ferrari, and J. Robertson, Phys. Rev. B **73**, 155426 (2006).
[30] G. D. Mahan, Phys. Rev. B **68**, 125409 (2003).
[31] J. Jiang, R. Saito, Ge. G. Samsonidze, S. G. Chou, A. Jorio, G. Dresselhaus, and M. S. Dresselhaus, Phys. Rev. B **72**, 235408 (2005).
[32] Valentin N. Popov, Luc Henrard, and Philippe Lambin, Phys. Rev. B **72**, 035436 (2005).
[33] Valentin N. Popov and Philippe Lambin, Phys. Rev. B **74**, 075415 (2006).
[34] C. T. White, D. H. Robertson, and J. W. Mintmire, Phys. Rev. B **47**, 5485 (1993).
[35] Ryan Barnett, Eugene Demler, and Efthimios Kaxiras, Phys. Rev. B **71**, 035429 (2005).
[36] C. T. White and T. N. Todorov, Nature (London) **323**, 240 (1998).
[37] In our calulations, we use the same related factors defined for the nearest and next nearest neighbors interactions in armchair CNTs by Mahan and Jeon. However, we prefer the notations $s_j^0=\sin(\theta_j/2)$, $c_j^0=\cos(\theta_j/2)$, $\tilde{s}^0=\sin(\tilde{\theta}/2)$, $\tilde{c}^0=\cos(\tilde{\theta}/2)$, $s_1^0=\sin(\theta_1/2)$, $s_2^0=\sin(\theta_2/2)$, $s_q^0=\sin qc$, $c_1^0=\cos(\theta_1/2)$, $c_2^0=\cos(\theta_2/2)$, $c_q^0=\cos qc$, and $\tilde{c}_\alpha^0=\cos(\alpha\tilde{\theta})$, $\tilde{s}_\alpha^0=\sin(\alpha\tilde{\theta})$. It should be noted that, since Eq. (24) in their paper is in this respect in misprint, the last two abbreviations differ from their notation.
[38] T. Altanhan and B. S. Kandemir, J. Phys.: Condens. Matter **5**, 6729 (1993).
[39] R. Wagner, *Unitary Transformations in Condensed Matter Physics* (Elsevier Science, Amsterdam, 1986).
[40] U. Fano, Phys. Rev. **124**, 1866 (1961); U. Fano and J. W. Cooper, Rev. Mod. Phys. **40**, 441 (1968).
[41] M. Abromowitz and I. A. Stegun, *Handbook of Mathematical Functions* (Dover, New York, 1972).
[42] R. W. D. Nickalls, Math. Gaz. **77**, 354 (1993).
[43] M. Damnjanović and M. Vujičić, Phys. Rev. B **25**, 6987 (1982).
[44] I. Milošević, R. Živanović, and M. Damnjanović, Polymer **38**, 4445 (1997).
[45] A. M. Rao, E. Richter, Shunji Bandow, Bruce Chase, P. C. Eklund, K. A. Williams, S. Fang, K. R. Subbaswamy, M. Menon, A. Thess, R. E. Smalley, G. Dresselhaus, and M. S. Dresselhaus, Science **275**, 187 (1997).
[46] C. Journet, W. K. Maser, P. Bernier, A. Loiseau, M. Lamy de la Chapelle, S. Lefrant, P. Deniard, R. Lee, and J. E. Fischer, Nature (London) **388**, 756 (1997).
[47] L. D. Landau and E. M. Lifschitz, *Quantum Mechanics: Non-relativistic Theory* (Pergamon, Oxford, 1977), pp. 300 and 380.
[48] M. Damnjanović, I. Milošević, E. Dobardžić, T. Vuković, and B. Nikolić, in *Applied Physics of Carbon Nanotubes*, edited by S. V. Rotkin and S. Subramoney (Springer, Berlin, 2005), pp. 41–85.
[49] Jean-Christophe Charlier, Xavier Blase, and Stephan Roche, Rev. Mod. Phys. **79**, 677 (2007).